Progress in Retinal and Eye Research 38 (2014) 43–69

Contents lists available at ScienceDirect

Progress in Retinal and Eye Research

journal homepage: www.elsevier.com/locate/prer

Grouped retinae and tapetal cups in some Teleostian fish: Occurrence, structure, and function

Mike Francke [a,b,1], Moritz Kreysing [c,1], Andreas Mack [d,1], Jacob Engelmann [e,1], Anett Karl [a,b,1], Felix Makarov [f,1], Jochen Guck [g,h,1], Mathias Kolle [i,1], Hartwig Wolburg [j,1], Roland Pusch [k,1], Gerhard von der Emde [k,1], Stefan Schuster [l,1], Hans-Joachim Wagner [d,1], Andreas Reichenbach [a,*,1]

[a] Paul-Flechsig-Institute of Brain Research, Leipzig University, Leipzig, Germany
[b] Translational Centre for regenerative Medicine, Leipzig University, Leipzig, Germany
[c] Dept. of Physics, Ludwig Maximilians University Munich, Munich, Germany
[d] Dept. Cellular Neurobiology, Institute of Anatomy, University Tuebingen, Tuebingen, Germany
[e] Dept. of Biology, AG Active Sensing, University Bielefeld, Bielefeld, Germany
[f] Pavlov Institute of Physiology, St. Petersburg, Russia
[g] Biotechnology Centre, Technical University Dresden, Dresden, Germany
[h] Cavendish Laboratory, Department of Physics, University of Cambridge, UK
[i] Harvard School of Engineering and Applied Sciences, Harvard University, Boston MA, USA
[j] Institute of Pathology and Neuropathology, University of Tuebingen, Tuebingen, Germany
[k] Institute of Zoology, University Bonn, Bonn, Germany
[l] Institute of Animal Physiology, University Bayreuth, Bayreuth, Germany

ARTICLE INFO

Article history:
Available online 22 October 2013

Keywords:
Grouped retina
Tapetum
Light reflection
Retinomotoric activity
Mesopic vision
Photonic crystals
Guanine
Behavioral adaptation

ABSTRACT

This article presents a summary and critical review of what is known about the 'grouped retina', a peculiar type of retinal organization in fish in which groups of photoreceptor cell inner and outer segments are arranged in spatially separated bundles. In most but not all cases, these bundles are embedded in light-reflective cups that are formed by the retinal pigment epithelial cells. These cups constitute a specialized type of retinal tapetum (i.e., they are biological 'mirrors' that cause eye shine) and appear to be optimized for different purposes in different fishes. Generally, the large retinal pigment epithelial cells are filled with light-reflecting photonic crystals that consist of guanine, uric acid, or pteridine depending on species, and which ensure that the incoming light becomes directed onto the photoreceptor outer segments. This structural specialization has so far been found in representatives of 17 fish families; of note, not all members of a given family must possess a grouped retina, and the 17 families are not all closely related to each other. In many cases (e.g., in Osteoglossomorpha and Aulopiformes) the inner surface of the cup is formed by three to four layers of strikingly regularly shaped and spaced guanine platelets acting as an optical multilayer. It has been estimated that this provides an up to 10fold increase of the incident light intensity. In certain deep-sea fish (many Aulopiformes and the Polymixidae), small groups of rods are embedded in such 'parabolic mirrors'; most likely, this is an adaptation to the extremely low light intensities available in their habitat. Some of these fishes additionally possess similar tapetal cups that surround individual cones and, very likely, also serve as amplifiers of the weak incident light. In the Osteoglossomorpha, however, that inhabit the turbid water of rivers or streams, the structure of the cups is more complex and undergoes adaptation-dependent changes. At dim daylight, probably representing the usual environmental conditions of the fish, the outer segments of up to 30 cone cells are placed at the bottom of the cup where light intensity is maximized. Strikingly, however, a large number of rod receptor cells are positioned behind each mirroring cup. This peculiar arrangement (i) allows vision at deep red wavelenghts, (ii) matches the sensitivity of rod and cone photoreceptors, and (iii) facilitates the detection of low-contrast and color-mixed stimuli, within the dim, turbid habitat. Thus, for these fish the grouped retina appears to aid in reliable and quick detection of large, fast moving, biologically relevant stimuli

Abbreviations: INL, inner nuclear layer; ONL, outer nuclear layer; OLM, outer limiting membrane; OS, outer segment(s); RGCs, retinal ganglion cells; RPE, retinal pigment epithelium.

* Corresponding author. Tel.: +49 0 341 9725731; fax: +49 0 341 9725739.
E-mail address: reia@medizin.uni-leipzig.de (A. Reichenbach).

[1] Percentage contribution of each author: MF, 10; MK, 5; AM, 5; JE, 5; AK, 5; FM, 5; JG, 5; MK, 5; HW, 5; RP, 5; GvdE, 5; SS, 5; HJW, 5; AR, 30.

1350-9462/$ – see front matter
http://dx.doi.org/10.1016/j.preteyeres.2013.10.001

such as predators. Overall, the grouped retina appears as a peculiar type of general retinal specialization in a variety of fish species that is adaptive in particular habitats such as turbid freshwater but also the deep-sea.

The authors were prompted to write this review by working on the retina of *Gnathonemus petersii*; the data resulting from this work (Landsberger et al., 2008; Kreying et al., 2012) are included in the present review.

Contents

1. Introduction

To understand the overwhelming diversity of retinal specializations among vertebrates has been – and still is – a continuous challenge not only to comparative anatomists (Schultze, 1866; Walls, 1963) but also to evolutionary biologists including Darwin himself (1859 he wrote, as an introduction to his explanation of the possible mechanisms of eye evolution, "To suppose that the eye with all its inimitable contrivances for adjusting the focus to different distances, for admitting different amounts of light, and for the correction of spherical and chromatic aberration, could have been formed by natural selection, seems, I freely confess, absurd in the highest degree"). In respect to the two basic types of photoreceptor cells, most retinae are specialized either for high-acuity (and color) vision at daylight – such as in the hawk eye and the primate fovea centralis, with high densities of (different spectral types of) cones – or toward high light sensitivity in dim environments – such as in some deep-sea fish and badgers, with a high density of rods (Walls, 1963; Reichenbach and Robinson, 1995; Lamb et al., 2007).

Generally, the vertebrate retina is composed of repetitive arrays ('microcolumns') of associated neuronal cells (Reichenbach and Robinson, 1995). This is most obvious in the case of the 'photoreceptor mosaics' in fish that consist of a species-specific assembly of distinct types of cone photoreceptor cells (Ali and Anctil, 1976, and references therein) plus a lifelong-increasing number of rod photoreceptor cells (Johns, 1982); these mosaics can certainly be associated with defined clusters of 'their' secondary and tertiary neurons completing the parallel retinal circuits. However, this pattern is not obvious in conventionally stained radial retinal sections, and is not subject of the present article. Rather, the article deals with very obvious structural associations of groups of photoreceptor cells with their adjacent, large retinal pigment epithelial (RPE) cells, resulting in bundles of photoreceptor cells collectively ensheathed by RPE 'cups'.

What now is called a 'grouped retina' in some fish was first observed about 100 years ago (Brauer, 1906). In such grouped retinae, which have since been found in quite a few fish species, all the photoreceptors in each bundle are thought to act together as one unified 'macroreceptor' (Locket, 1971; Kreysing et al., 2012). Obviously, this organization is incompatible with high spatial resolution (Schuster and Amtsfeld, 2002); it was thus concluded that it must be a straightforward adaptation to dim-light vision (Locket, 1971; Schuster and Amtsfeld, 2002). However, it was recently shown that this is only half the truth: in the case of the Elephantnose fish *Gnathonemus petersii* the grouped retina is definitely not optimized for maximizing photon catch by rod photoreceptors (Kreysing et al., 2012). This review is aimed at an elucidation of the design and function of different types of grouped retinae in diverse fish living in different habitats, on the basis of the available literature.

2. Discovery of the grouped retina – a short history

Having explored the material provided by the German deep-sea expedition 'Valdivia' 1898–1899, Brauer published his impressive work on the anatomy of deep-sea fishes (Brauer, 1906). In the chapter "Die Augen von bathypelagischen Fischen" ("The eyes of bathypelagic fishes") he showed, for the first time, the histological appearance of a grouped retina (Fig. 1A). Two decades later, a similar retinal anatomy was described by Franz (1921) in a freshwater-fish (Mormyrid) retina (Fig. 1B).

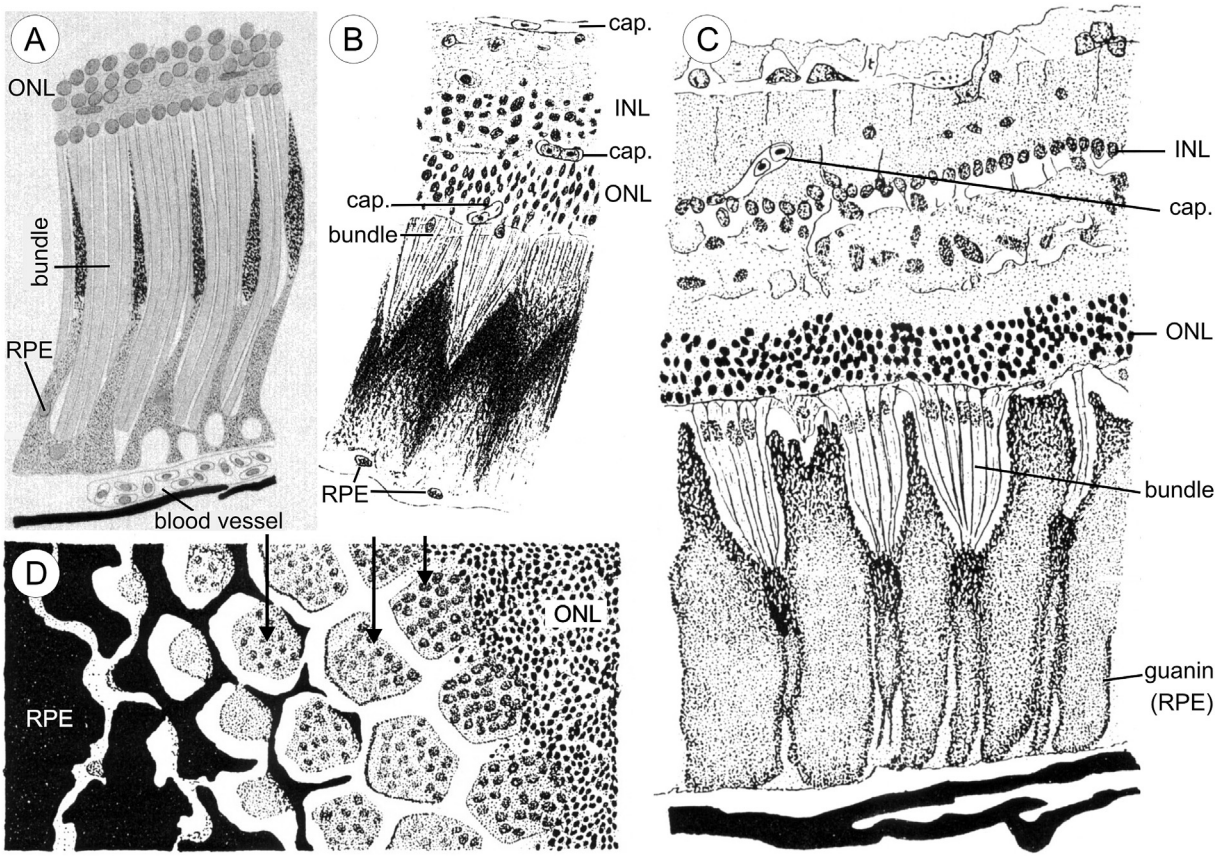

Fig. 1. Historical drawings of grouped retinae by Brauer (1906) (A), Franz, 1921 (B) and McEwan, 1938 (C, D). Radial retinal sections (A–C) and slightly oblique transversal section through the outer retina (D). Bundles (see also *arrows* in D) of photoreceptor cell inner and outer segments are shown in a deep-sea fish (A) and in Mormyrid fish (B–D). INL, inner nuclear layer; ONL, outer nuclear layer; RPE, retinal pigment epithelium, cap, capillaries.

Whereas Brauer (1906) and Franz (1921) just showed or shortly mentioned these photoreceptor cell bundles, McEwan (1938) explicitly devoted her work to "study the retinae of some of the Mormyridae more accurately and to compare the structure with that of other Teleosts..." (McEwan, 1938). Her work provided the first detailed explanation of the peculiarities of the Mormyrid retina, revealing the complex interrelationship between photoreceptor cell bundles and the guanine crystal-containing RPE cells. She also pointed to the fact that the fish are "living in the shady parts or on the muddy bottom of the stream" and concluded that in "the dimly lit waters... all the available light would need to be conserved and the guanine would serve to throw back the light into the visual elements" (McEwan, 1938). A few years later, Moore (1944) studied a North American 'distant relative' of the African Mormyrids, *Hiodon tergisus*. He found a very similar retina structure but came to a completely different conclusion, viz. that it provides "a shielding of the rod outer segments from bright light" (Moore, 1944). Recently his conclusion was confirmed, but the apparently contradictory suggestion of McEwan was confirmed as well – with the modification that available light intensity is enhanced for the cones, rather than for the rods (Kreysing et al., 2012; and see Section 5.1). Back to history, however, it is noteworthy that there was another discrepancy between the observations of the two authors. Whereas McEwan wrote that "…the Mormyrid retina shows… little change when exposed to various light intensities" Moore already noted that "Hiodon possesses light-adaptive photomechanical changes". As will be shown later (Section 4.3, Fig. 3A and B, 5, and 10), the complex cups of Osteoglossiform fish (to which both the Mormyrids and the Hiodontines belong) all display retinomotor adjustments of the rods (and the cup walls) but not necessarily also of the cones. Although these two articles left a number of open questions, two decades passed before other authors studied grouped fish retinae, often then by using electron microscopy (Engström, 1963; O'Connel, 1963; Munk, 1966, 1975, 1977; Locket, 1971, 1977; Zyznar, 1975; Zyznar and Ali, 1975; Zyznar et al., 1978; Frederiksen, 1976; Wagner and Ali, 1978; Best and Nicol, 1979). In fact, the term "grouped retina" was first introduced by Locket (1971, 1977). Since then, the fascination of the grouped retina has attracted many researchers, and still does (e.g., Braekevelt, 1982; Kunz et al., 1985; Munk, 1989; Braekevelt et al., 1989; Somiya, 1980, 1989; Collin et al., 1998; Awaiwanont et al., 2001; Nag, 2004; Taylor and Grace, 2005; Heß et al., 2006; Novales Flamarique, 2011; Kreysing et al., 2012). This has led to the generation of much data but not to any comprehensive understanding of the structure and its function. Many articles are not easily accessible, and reviews are only available for the grouped retina of deep-sea fish retinae (Locket, 1977; Douglas et al., 1998; Warrant and Locket, 2004) or have been written before the more recent data were published (Zyznar, 1975). This prompted us to compile the known data, and to review them in the light of current ideas and approaches.

3. Appearance of the grouped retina

3.1. Occurrence among different families of teleosts

Grouped retinae have been described in representatives of seventeen out of the more than seventy (Nelson, 2006) known Teleostean fish families, including the Mormyridae (freshwater elephantfish), Gymnarchidae (knifefish), Notopteridae (featherbacks), Hiodontidae (mooneyes), Megalopidae (tarpons), Engraulidae (anchovies), Clupidae (herrings), Pristigasteridae (longfin herrings),

Table 1
Summary of the known fish species possessing a grouped retina, with an indication of their habitats and of the type of tapetal cups present. Note that *Trachinus vipera* is exceptional in having a grouped retina but no tapetal cup (**X**). PD = platelet covered duplex cup (cones and rods); PD* = platelet covered duplex cup (cones and rods + twin cones); SD = simple-crystal duplex cup (cones and rods); PR = platelet covered rod-only cup; PC = platelet covered cone-only cup (cf. Fig. 3 for explanation of the cup types). References are, 1. Ali and Anctil (1976); 2. Awaiwanont et al. (2001); 3. Best and Nicol (1979); 4. Braekevelt (1982); 5. Braekevelt et al. (1989); 6. Brauer (1906); 7.Collin et al. (1998); 8. Engström (1963); 9. Franz (1921); 10. Frederiksen (1976); 11. Heβ et al. (2006); 12. Kreysing et al. (2012) 13. Kunz et al. (1985); 14. Locket (1971); 15. Locket (1977); 16. McEwan (1938); 17. Moore (1944); 18. Munk (1966); 19. Munk (1975); 20. Munk (1977); 21. Munk (1989); 22. Nag (2004); 23. Novales Flamarique (2011); 24. O'Connell (1963); 25. Somiya (1980); 26. Somiya (1989); 27. Taylor and Grace (2005); 28. Wagner and Ali (1978); 29. Zyznar (1975); 30. Zyznar and Ali (1975); 31. Zyznar et al. (1978); 32. present paper, Fig. 6.

Higher taxon	Family	Genus	Species	Habitat	cup type	Ref.
Osteoglossi-formes	Mormyridae	*Gnathonemus*	*petersii*	Turbid Freshwater	PD	12, 16, 26
			macrilepidotus	Turbid freshw.	PD	16
		Petrocephalus	*stuhlmanni*	Turbid freshw.	PD	16
			Brevipedunculatus	Turbid freshw.	PD	8
		Marcusenius	*rudebeckeri*	Turbid freshw.	PD	8
			longianalis	Turbid freshw.	PD	9, 26
			isidori	Turbid freshw.	PD	26
		Mormyrus	*rume ssp. proboscirostris*	Turbid freshw.	PD	32
	Gymnarchidae	*Gymnarchus*	*niloticus*	Turbid freshw.	PD	8
	Notopteridae	*Notopterus*	*notopterus*	Turbid freshw.	PD	1, 22
		Xenomystes	*nigri*	Turbid freshw.	PD	1
	Hiodontinae	*Hiodon*	*alosoides*	Turbid freshw.	PD	3, 4, 28, 31
			tergesius	Turbid freshw.	PD	18, 28, 31
Elopiformes	Megalopidae	*Megalops*	*cyprinoides*	Pelagic murky	PD	16
			atlanticus	Marine/freshwater brackish	PD	16, 27
		Elops	*saurus*	Marine brackish	PD	16, 27
Clupeiformes	Engraulidae	*Engraulis*	*japonicus*	Neritic turbid	PD*	2, 23
			mordax	Neritic turbid	PD*	11, 24
		Lycothrissa	*crocodilus*	Turbid	PD*	11
	Clupidae	*Dorosoma*	*cepedianum*	Marine/freshwater brackish	(SD)	29
	Pristigasteridae	*Ilisha*	*africana*	Marine brackish	(SD)	11
Perciformes	Percidae	*Stizostedion*	*vitreum*	Freshw. brackish	SD	5, 30
	Trachinidae	***Trachinus***	***vipera***	**Benthic murky**	**none**	**13**
Beryciformes	Polymixiidae	*Polymixia*	*japonica*	Deep-sea	PR	25
			berndti	Deep-sea	PR	25
Aulopiiformes	Paralepidae	*Notolepis*	*rissoi*	Deep-sea	PR PC	15
		Lesidiops	*affinis*	Deep-sea	PR PC	21
	Scopelarchiae	*Scopelarchus*	*güntheri*	Deep-sea	PR	14, 15
			sagax	Deep-sea	PR	14
			michaelsarsi	Deep-sea	PR PD	7
			analis	Deep-sea	PR	7
		Benthabella	*infans*	Deep-sea	PR	15
	Scopelosauri-dae	*Scopelosaurus*	*lepidus*	Deep-sea	PR PC	20
			hoedti	Deep-sea	PC	19
		Ahliesaurus	*berryi*	Deep-sea	PC	19
	Chlorophthal-midae	*Chlorophthalmus*	*albatrossi*	Deep-sea	PR	25
			nigromarginatus	Deep-sea	PR	25
			acutifrons	Deep-sea	PR	25
	Evermannelli-dae	*Evermanella*	*indica*	Deep-sea	PR	6, 18
			atrata	Deep-sea	PR	6
	Omosudidae	*Omosudis*	*lowei*	Deep-sea		10

Percidae (perches), Trachinidae (weeverfish), Polymixidae (beardfishes), Paralepidae (barracudinas), Scopelarchidae (pearleyes), Scopelosauridae (waryfishes), Chlorophthalmidae (greeneyes), Evermannellidae (sabertooth fishes), and Osmosudidae (hammerjaws). As shown in Table 1 and Fig. 2, some but by no means all of these families are closely related to each other. Moreover, of the about 40 fish species known to possess a grouped retina, some appear to be 'typical representatives' of their phyla (e.g., all Osteoglossomorpha studied so far possess a grouped retina) whereas others seem to be exceptions among their relatives (e.g., most Clupidae possess a conventional retina). We cannot exclude that grouped retinae may be found in other families of fish (and certainly they will be detected in more species belonging to the above-mentioned families). Noteworthy, grouped retinae have exclusively been found in teleost fish and in no other vertebrate phylum.

3.2. Different types of structural organization

Whereas Fig. 1 emphasizes the basic similarity between grouped retinae with tapetal cups in deep-sea fish and Mormyrids, a closer inspection reveals a number of differences. All (?) Mormyridae and a number of other Osteoglossiformes, as well as some Megalopidae, Engraulidae, and Clupidae have a grouped retina in which the photoreceptor cell bundles contain both rods and cones; these retinae display retinomotor activity during dark- *vs.* light adaptation (Figs. 3A, B and 10). A variety of deep-sea fishes (many Aulopiformes and some Bercyformes) possess retinae or retinal regions in which groups of rod photoreceptors form spatially separated bundles (Fig. 3E–G).

These two basic types of grouped retinae may be modified in some species. In some anchovies, the photoreceptors are arranged in rows separated by tapetal 'curtains' which allows for the detection of polarized light (Fig. 3H–K). For instance, the retina of *Engraulis japonicus* contains two different types of cones and, accordingly, particularly complex-shaped tapetal platelet arrangements (Fig. 3J, K) (Awaiwanoni et al., 2001; Novales Flamarique, 2011) and thus may be considered as representing the highest known degree of structural specialization. At the other end of the scale, the retina of *Stizostedion vitreum* contains photoreceptor bundles quite similar to those of the mormyrids but the ensheathing tapetal cup contains only irregularly-shaped reflective

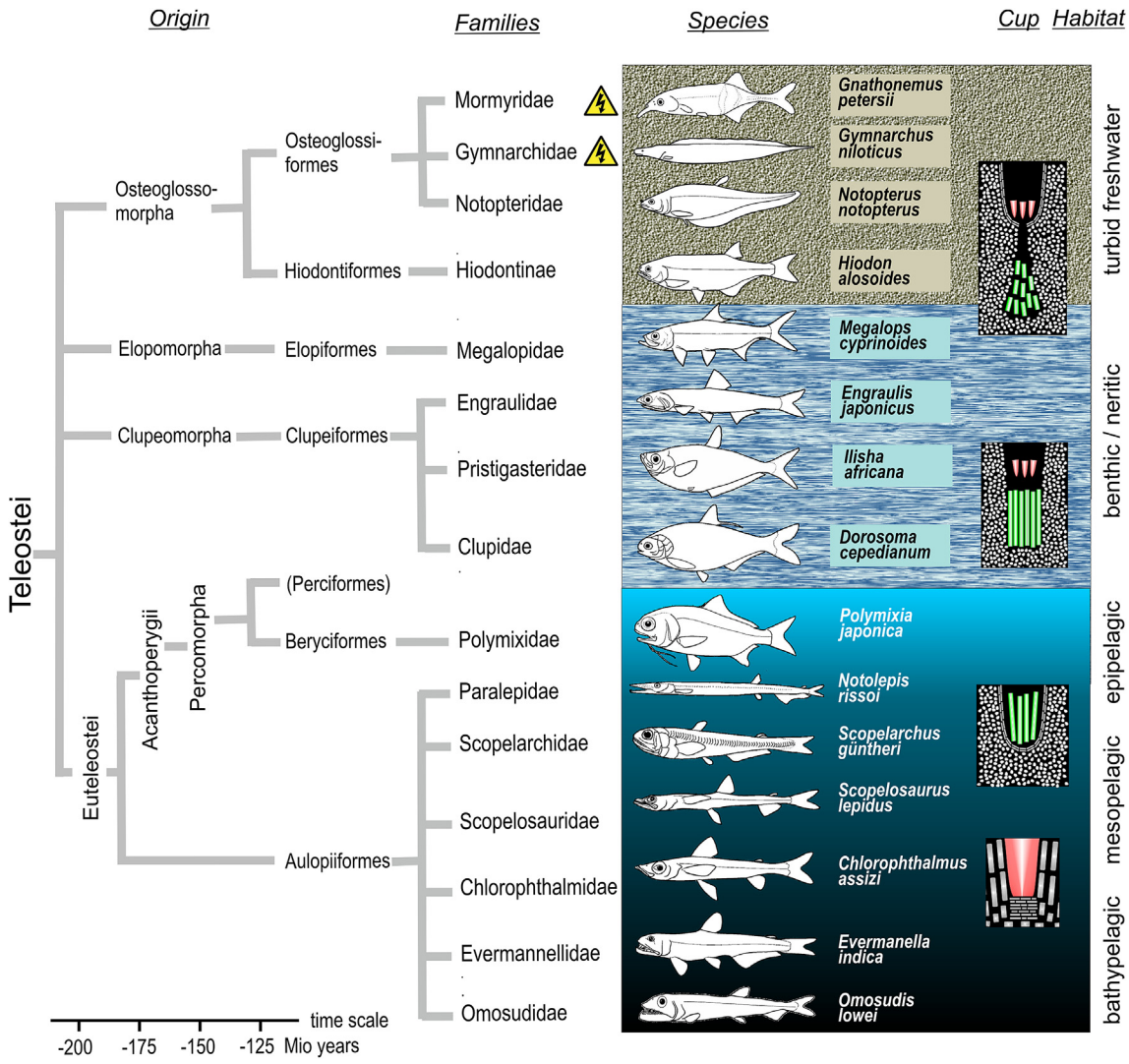

Fig. 2. Survey of the occurrence of grouped retinae among Teleostean fishes. The raw 'phylogenetic tree' is based upon Nelson (2006), and the raw time scale was adjusted according to Davis and Fielitz (2010). The meaning of the symbols for the different types of tapetal cups will be explained in Fig. 4; the electricity signs indicate that the fish possess an active electric sense. For the meaning of the cup symbols, see Fig. 5. Note that representatives of the Perciformes are not shown in the drawing, for the sake of clarity (*cf.* Table 1).

crystals, rather than additional layers of platelet-shaped crystals at its surface as in the other fishes (Fig. 5) (Zyznar and Ali, 1975; Braekevelt, 1982). This type of grouped retina may thus be considered as representing the lower end of the scale of tapetal differentiation. It is of interest to note but difficult to explain that in *Trachinus vipera*, bundles of photoreceptors have been observed but these are not surrounded by tapetal cups (Kuntz et al., 1985).

Among the deep-sea fishes with grouped retinae, a special case is constituted by some species in which there are retinal areas with cone photoreceptor cells; their outer segments are also embedded in tapetal cups (Fig. 4E, F). The structure and ultrastructure of these cups differs remarkably from those enveloping the groups of rods (Figs. 4F and 5) (Frederiksen, 1976). Whereas generally the cups in freshwater fishes and the rod-embedding cups in the deep-sea fishes resemble parabolic mirrors in their shape, and display a similar ultrastructure at their walls and bottom (see Section 5), the cone-surrounding cups contain stacks of flat platelet-shaped crystals at their bottom but larger, rod-shaped crystals in their walls (Figs. 4E–F, 5) (Frederiksen, 1976).

Taken together, the following five types of photoreceptor bundles can be defined (Fig. 5), with platelet-covered duplex cups, with 'simple' duplex cups, and without cup (all in freshwater fishes) and rod-only and cone-only cups (in deep-sea fishes). More about the optical properties of the reflecting cups will be presented later (section 5).

3.3. Phylogenesis and ontogenesis

Although a raw 'phylogenetic tree' of the involved fishes is presented in Fig. 2, the relationships between the fish groups and (times of) their origins are just beginning to be resolved (e.g., Davis and Fielitz, 2010). Nonetheless, current knowledge allows some speculations about the origin(s) of the grouped retinae and their tapetal cups. It seems reasonable to assume that some early Osteoglossiformes, probably already occupying turbid freshwaters, developed the duplex cups as an adaptation to these 'uncomfortable' habitats. Once established, this retinal specialization may have been maintained by their descendants, and, in turn, may have enabled them to occupy – and live in – such habitats. Clearly, this retinal specialization is not correlated with an electric sense, as only two of the families include weakly electric fish (Fig. 2).

It is more difficult to hypothesize about a possible common origin of the grouped retinae and tapetal cups in the

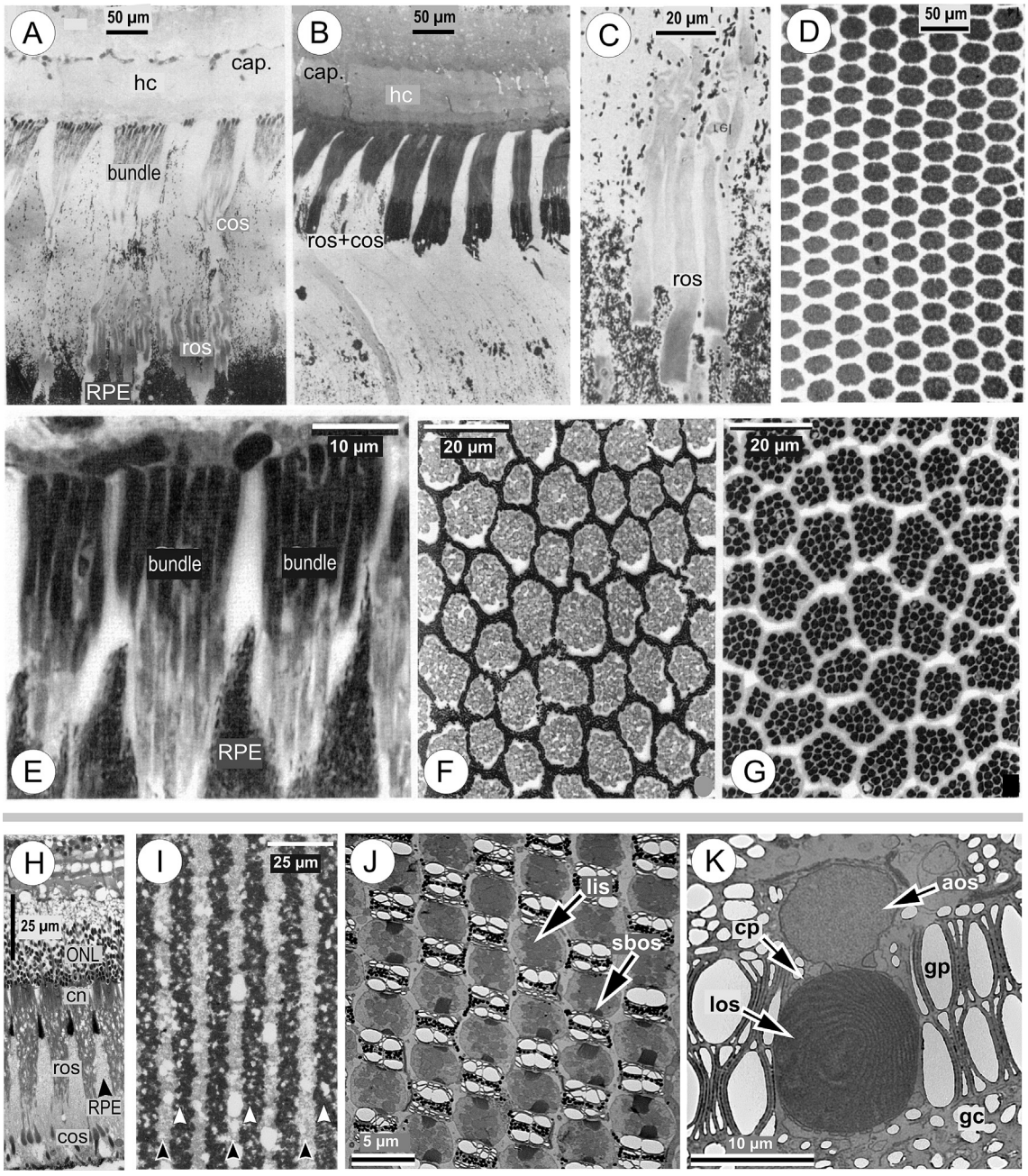

Fig. 3. Examples of the histological structure of grouped retinae in fishes. **A**–**D**, radial (**A**–**C**) and tangential (**D**) sections through the retina of a freshwater fish, the mooneye (*Hiodon tergisus*). The photoreceptor cell bundles are clearly visible both in the light-adapted (**A** and **C**) and dark-adated retina (**B**) but the level at which the rod outer segments (ros) are located changes considerably (cf. also Fig. 10). In tangential sections the strikingly regular arrangement of the bundles becomes obvious (**D**). **E**–**G**, radial (**E**) and tangential (**F, G**) sections through the accessory retina of a deep-sea fish, *Scopelarchus michaelsarsi*. Rod-like photoreceptors are bundled in the dorsal part of the accessory retina, and embedded in tapetal cups formed by the retinal pigment epithelium (RPE). This involves not only the outer segments (**F**) but even the cell nuclei in the outer nuclear layer (**G**). **H**–**K,** Special arrangement of rows of photoreceptors and wedge-shaped RPE cell processes in the anchovy retina (**H, I,** *Ilisha africana*; **J, K**, *Engraulis mordax*). **H**, If the retina is cut perpendicular to the rows, the structure is reminescent of that of the cups observed in the Mormyrids. In tangential sections or wholemounts (**I**), however, it becomes apparent that the PRE processes, filled with different types of crystallites, form long 'curtains' (black arrowheads) between rows of two different types of cones (white arrowheads). **J**, **K**, Different cones (aos, accessory cone outer segment; lis, long cone inner segment; los, long cone outer segment; sbos, short cone bilobed outer segment) are arranged in rows, flanked by guanine platelet stacks (gp) and guanine crystals (gc). cn, cone nuclei; cos, cone outer segment; cp, calycal process; ONL, outer nuclear layer; ros, rod outer segments. Modified from Wagner and Ali (1978) (A–D) Collin et al. (1998) (E–G), Heß et al. (2006) (H, I) and Novales Flamarique (2011) (J, K).

Osteoglossiformes and other freshwater fishes. The occurrence of 'imperfect' (*Stizostedion*) and even missing cups (*Trachinus*) in some grouped retinae may indicate that these species are just in the process of establishing this retinal specialization which would argue for an independent origin. Of course, it cannot be excluded that these forms are indications of decomposing a formerly well-developed structure. Recently, the evolution of 'polycones' separated by long pigment epithelium barriers containing tapetal crystallites (Heß et al., 2006) in Achovy retinae has been studied, and used as an aid for reconstruction of engraulidid phylogeny (Heß et al., 2006). Clearly this argues for an independent evolution of similar retinal specializations in this group of fishes.

Also in the case of deep-sea fishes, an independent origin of the grouped retinae/tapetal cups appears very likely, as these species

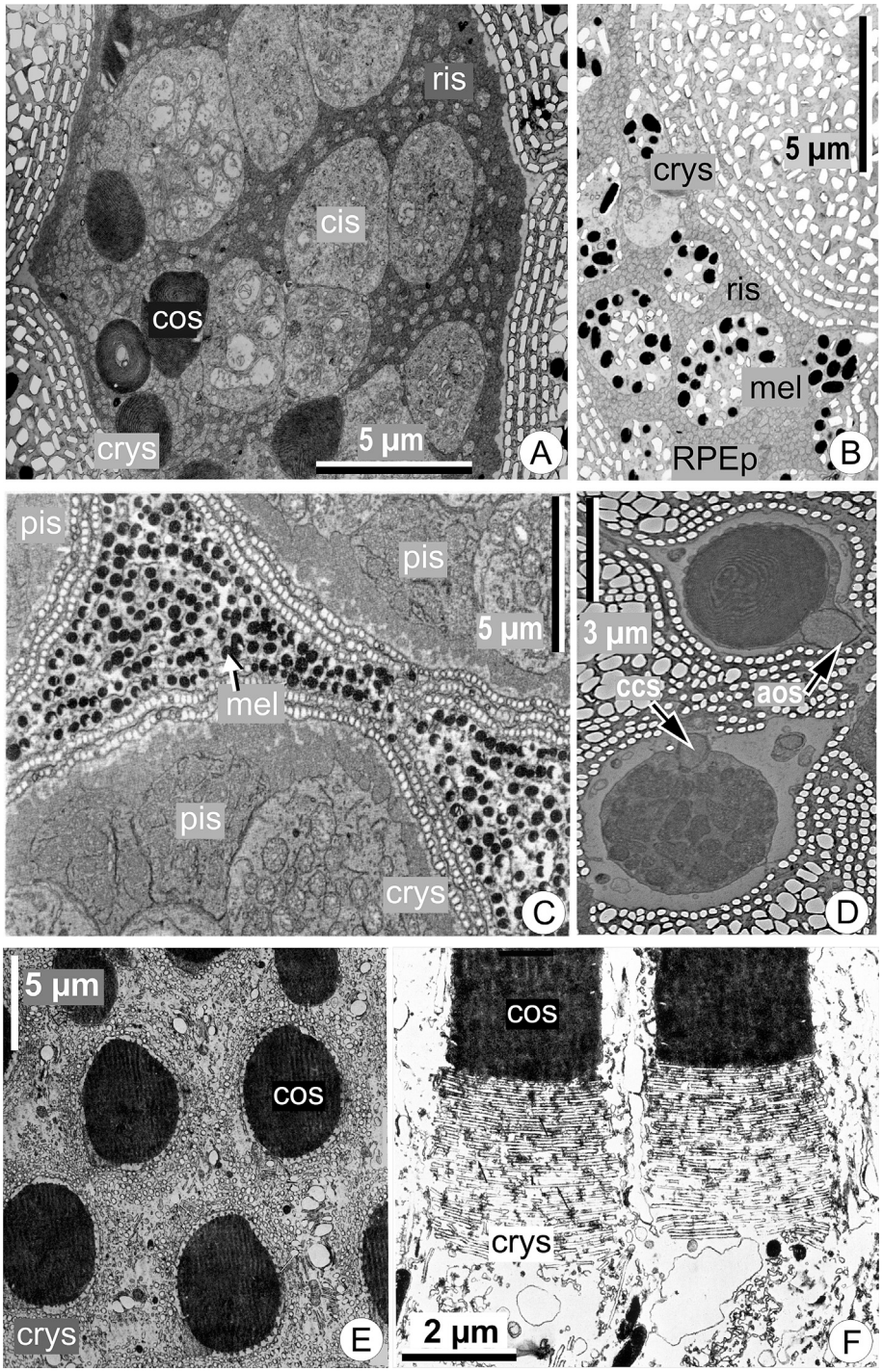

Fig. 4. Examples of the ultrastructure of the tapetal cups in fishes. **A**–**D**, tangential ultrathin sections through the retina of the freshwater fishes, *Gnathonemus petersii* (**A, B**) and *Hiodon alosoides* (**C**) It is apparent that in all these retinae, the surface of the cups is constituted by three or four rather regularly arranged layers of (platelet-like) crystals (crys). This applies to the entire surface of the cup from margin (cf. Fig. 13) via the bottom-near region where the cone inner segments (cis) give rise to the outer segments (cos) (**A**) up to the very bottom where only the rod inner segments (ris) run further down and are met by the tips of processes of the retinal pigment epithelium (RPEp) (**B**). **D**, Similar crystalline structures surround individual cones in the centrodorsal retina of the anchovy, *Engraulis mordax*. **E, F**, tangential (**E**) and radial (**F**) ultrathin sections through the cone-containing retina of the deep-sea fish, *Omosudis lowei*. The cone outer segments (cos) are surrounded by a multiplayer of rod-shaped crystals (**E**) but at their tips there are stacks of flat, platelet-shaped crystals (**F**). aos, accessory outer segment; ccs, connecting ciliar structure; pis, photoreceptor cell inner segments; mel, melatonin granules. **A, B**, originals; **C**–**F** modified from Braekevelt (1982) (**C**), Novales Flamarique (**D**) and Frederiksen, 1976 (**E, F**).

are very distantly related to the Osteoglossiformes and the other freshwater fishes with grouped retinae, and developed much later than these (Fig. 2). Thus, we favor the conclusion that this retinal specialization arose at least twice (probably more often) in fish evolution. This might have been due to a common environmental pressure, *viz*. the need for increased light delivery in dark habitats and/or turbid water (cf. Sections 5–7).

The embryonic development of the grouped retinae is poorly studied. In *Stizostedion vitreum* (i.e., the species with a 'simple' duplex cup) this specialization develops late, together with the

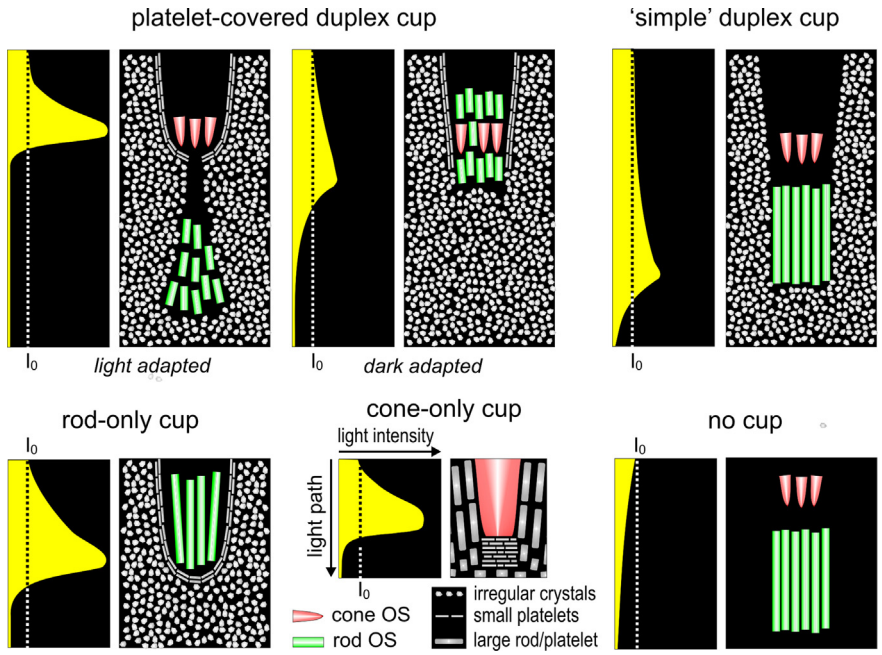

Fig. 5. Different types of grouped retinae/tapetal cups in fishes (cf. also Figs. 3 and 4). OS, outer segments. (The schematic drawings presented here are also used as symbols in Fig. 2).

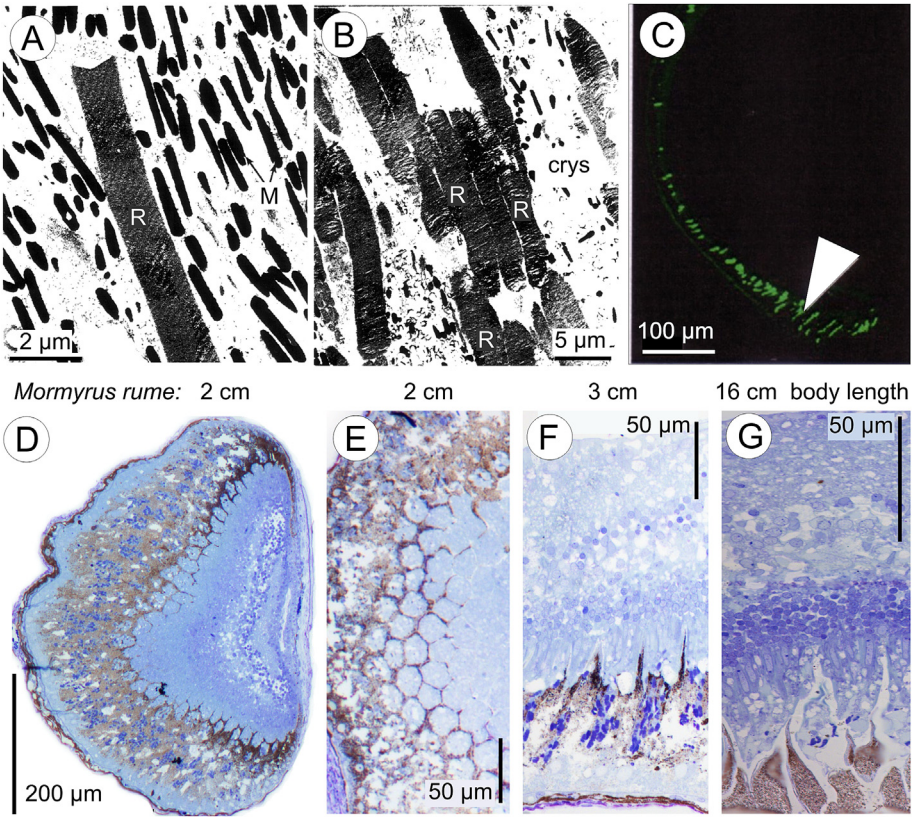

Fig. 6. Developmental stages of the structure of grouped retinae in different fish. **A, B**, Electron microscopic images of rods (R) and their surrounding retinal pigment epithelial cells in a young (5 cm body length) (**A**) and slightly older (6 cm body length) walleye (*Stizostedion vitreum vitreum*) (**B**). Grouping of the rods and appearance of tapetal crystals (crys) are found only the older stage. **C**, immunohistochemical photograph of a section through the retina of a young (settlement-stage) *Elops saurus*; individual rods are labeled by a rod-specific antibody (arrowhead). **D**–**G**, Histological sections through an eye (**D**) and the retinae (**E**–**F**) of *Mormyrus rume proboscirostris* fish of different developmental stages as indicated by the body length data on top of the images. Bundles of rods and tapetal cups are established in all stages studied. M, melanin granules. **A**–**B**, Modified from Braekevelt et al. (1989); **C**, modified from Taylor and Grace (2005); **D**–**G**, originals (H–J W).

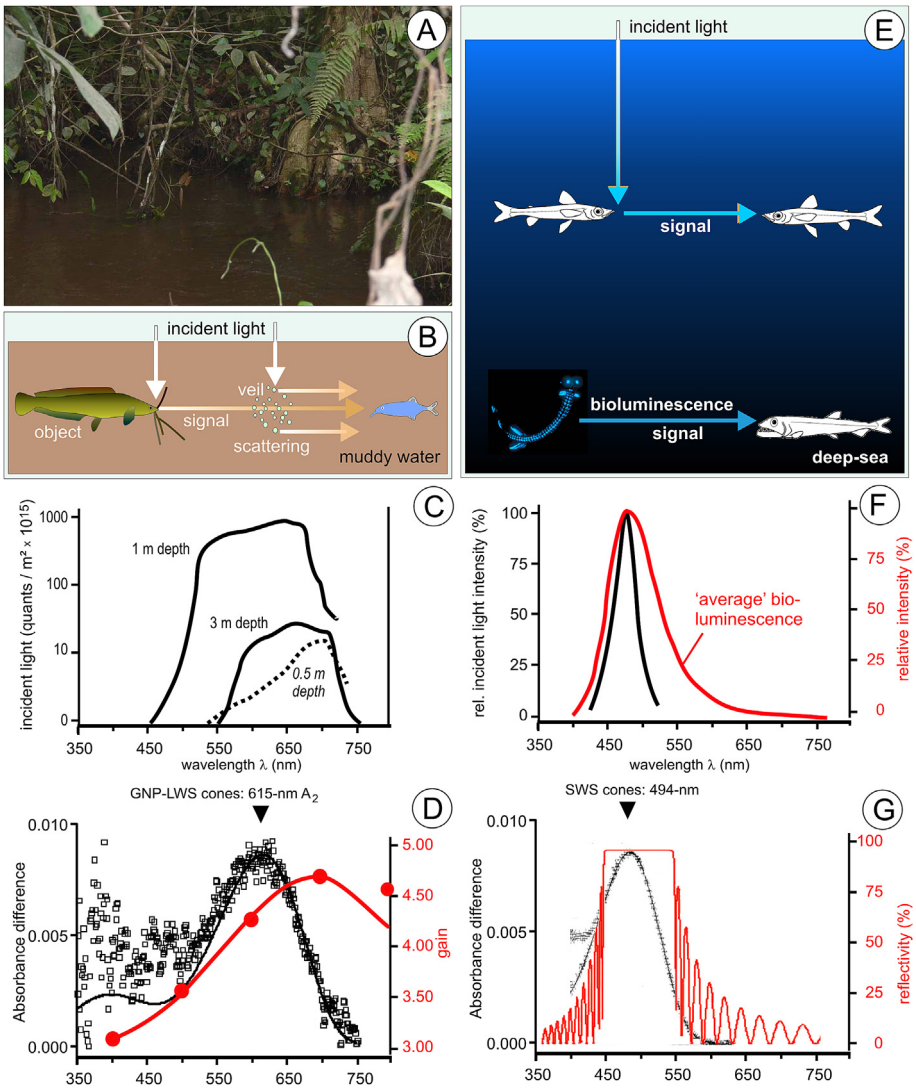

Fig. 7. Habitats of Mormyrid (**A**–**C**) and deep-sea fishes (**E, F**), and their retinal adaptations (**D** and **G**), respectively. (**A**), Habitat of *Gnathonemus petersii*. In the Iguidi river in Benin, a relatively fast moving creek which flows through the forest, during daytime *G. petersii* only occurs in areas shaded by trees (with permission from Vivica von Vietinghoff). (**B**), Schematic illustration of the impact of absorption and scattering in the turbid, blackwater habitat of *Gnathonemus*. For explanation, please refer to text. (**C**), Spectral distribution of underwater light in turbid waters in Southern Africa (solid lines: Walmsely et al., 1980) and of underwater light in Lake Burley Griffin (AUS) under highly turbid conditions (69 NTU; dotted line: Kirk, 1985). (**D**), Wavelength-dependence of the light intensity enhancement for the COS at the cup bottom of *Gnathonemus* simulated by an electrodynamical model (*red line; cf.* Figs. 14E and 15) and absorption spectrum of isolated outer segments of cones (*squares*); the solid line represents the corresponding Dartnall diagram (modified from Kreysing et al., 2012). (**E**), Schematic illustration of the impact of absorption of light in the deep-sea. For explanation, please refer to text. (**F**), Spectral distribution of underwater light in the deep-sea at 300 m depth (*black line*: modified from Warrant and Locket, 2004) and of bioluminescence averaged from a number of bioluminecent deep-sea animals (*red line*: calculated from data given by Johnsen et al., 2012). (**G**), Wavelength-dependence of the light reflectivity of the cup bottom to the COS simulated by an electrodynamical model (*red line*; cf. Fig. 16) and absorption spectrum of isolated outer segments of cone-like photoreceptors of *Scopelarchus* (*squares*); the solid line represents the corresponding Dartnall diagram (modified from Partridge et al., 1992; Pointer et al., 2007).

tapetal crystals (Braekevelt et al., 1989). In young fish with a body length of less than about 5 cm, the rods are not grouped but are aligned as individual entities, and the retinal pigment epithelium contains melanin granules but no reflective crystals (Fig. 6A). When a body length of 6 cm is achieved, the rods of the fish are bundled and surrounded by pigment epithelial processes that contain crystals (Fig. 6B). A similar, rather rapid 'switch' of retinal organization has been described for the *Megalops atlanticus* and *Elops saurus*, two species with a 'perfect' platelet-covered duplex cup. Larval fish at the settlement stage still display single, scattered rods (Fig. 6C) and – to the best of our knowledge – no reflective tapetum (Taylor and Grace, 2005). Soon after settlement, the juvenile fish then possess a well-developed grouped retina with tapetal cups (Taylor and Grace, 2005). In the Mormyrids, very young developmental stages are hardly available; noteworthy, however, even small *Mormyrus rume* fish of 2 cm body length already display a well-developed retinal specialization (Fig. 6D–G)

Very likely, a (hitherto unknown) developmentally regulated mutual signaling process between the RPE and the (rod) photoreceptor cells induces the bundling and the expression of tapetal crystals simultaneously in embryonic development, although the time of this induction appears to vary among the different species.

4. A well-studied example: the retina of *Gnathonemus petersii*

4.1. Habitat and basic behavior of the fish

The Elephantnose fish, *Gnathonemus petersii*, is probably the best-studied member of the African Mormyridae, mainly because its ability to produce and to sense weak electric signals has long

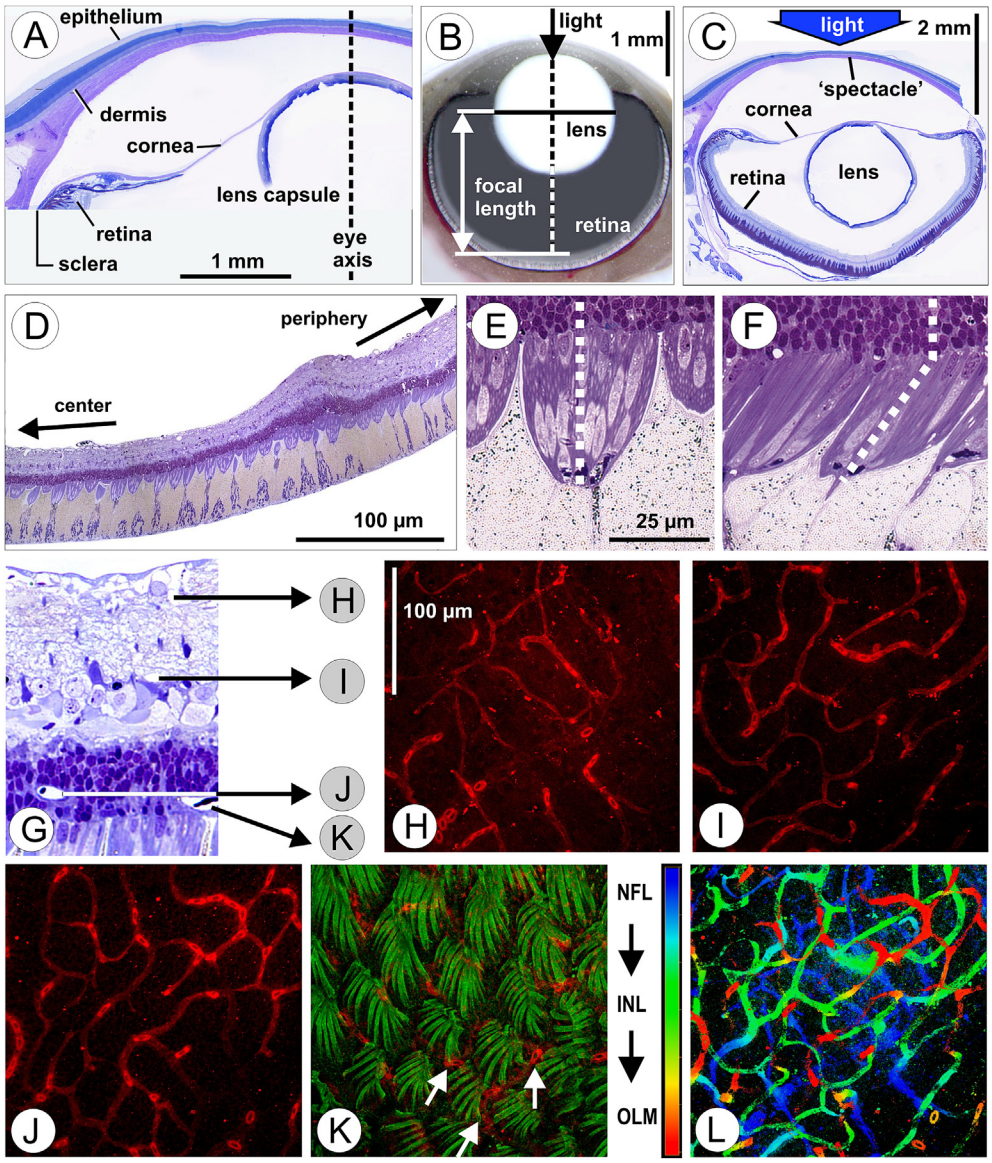

Fig. 8. Special features of the *Gnathonemus* eye (**A**–**C**) and retina (**D**–**L**). **A**, Anterior part of a transversal section through an adult eye. Both the cornea and the sclera are thin but the eye is covered by a dermal 'spectacle'. **B**, A cryosection through an unfixed eye reveals that the cleft between the cornea and the spectacle is artificial. Eye and leans are roughly spherically shaped, and the focal length of the eye can easily be measured (about 2–3 mm, depending on fish size). **C**, Section through an entire adult eye, with a higher-magnified part of the retina shown in **D**. Obviously, the orientation of the bundles to the retinal surface is not constant in different retinal areas; they are orthogonally oriented in the retinal center (**E**) but obliquely in the periphery (**F**). **G**–**H**, Intraretinal blood vessels occur at three distinct levels, in the ganglion cell layer (**H**), inner plexiform layer (**I**), and outer nuclear layer, close to the external limiting membrane (**J, K**). The arrows in (G) indicate the levels where the images (H–K) were obtained. Blood vessels were detected by their auto-fluorescence in the paraformaldehyde-fixed retinae (**H**–**K**, *red*), cones were counter-labeled by a mouse monoclonal antibody, T7, staining cone arrestin in other teleosts (Mack, 2007) (**K**, *green*). **L**, Merge of images of blood vessels in all layers; the color codes for the depth of the confocal recordings. The calibration bar in (H) is valid for (H–L).

been known and studied by many researchers. Like all weakly electric Mormyrids, *G. petersii* uses its electric organ discharges (EODs) for electro-communication with conspecifics (e. g., Hopkins, 2009) and for probing its environment to detect and analyze objects in its vicinity, a process called active electro-location (e. g., Von der Emde et al., 2010). During each EOD an electrical field builds up in the water around the fish. This self-produced field is perceived by an array of more than 2000 epidermal electroreceptor organs distributed all over the body surface of the fish. Nearby objects are detected because they distort the fish's electrical field and thus change the input to the electroreceptors. The operating distance of this sensory system is limited (see below).

G. petersii lives in small creeks and rivers of Central and West Africa, where – at least seasonally – floods might cause a high turbidity of the water (Moller, 1995). The major freshwater habitat types inhabited by *G. petersii* are moist forest rivers, but they were also found in Savanna-dry forest rivers as well as in floodplains, swamps and lakes and large river deltas (Moritz, 2010; Paugy et al., 1994; Nwani et al., 2011). Common features of all these habitats are relatively low light levels because of shade provided by tree and bush cover, a reddish color of the water, and often rather fast flowing currents. The water has temperatures above 25 °C. A typical habitat is the Iguidi River, a small forest stream in South-East Benin (Fig. 7A). Here and at other sampling sites, *G. petersii* was regularly observed within fast flowing parts of the river (e. g., under roots

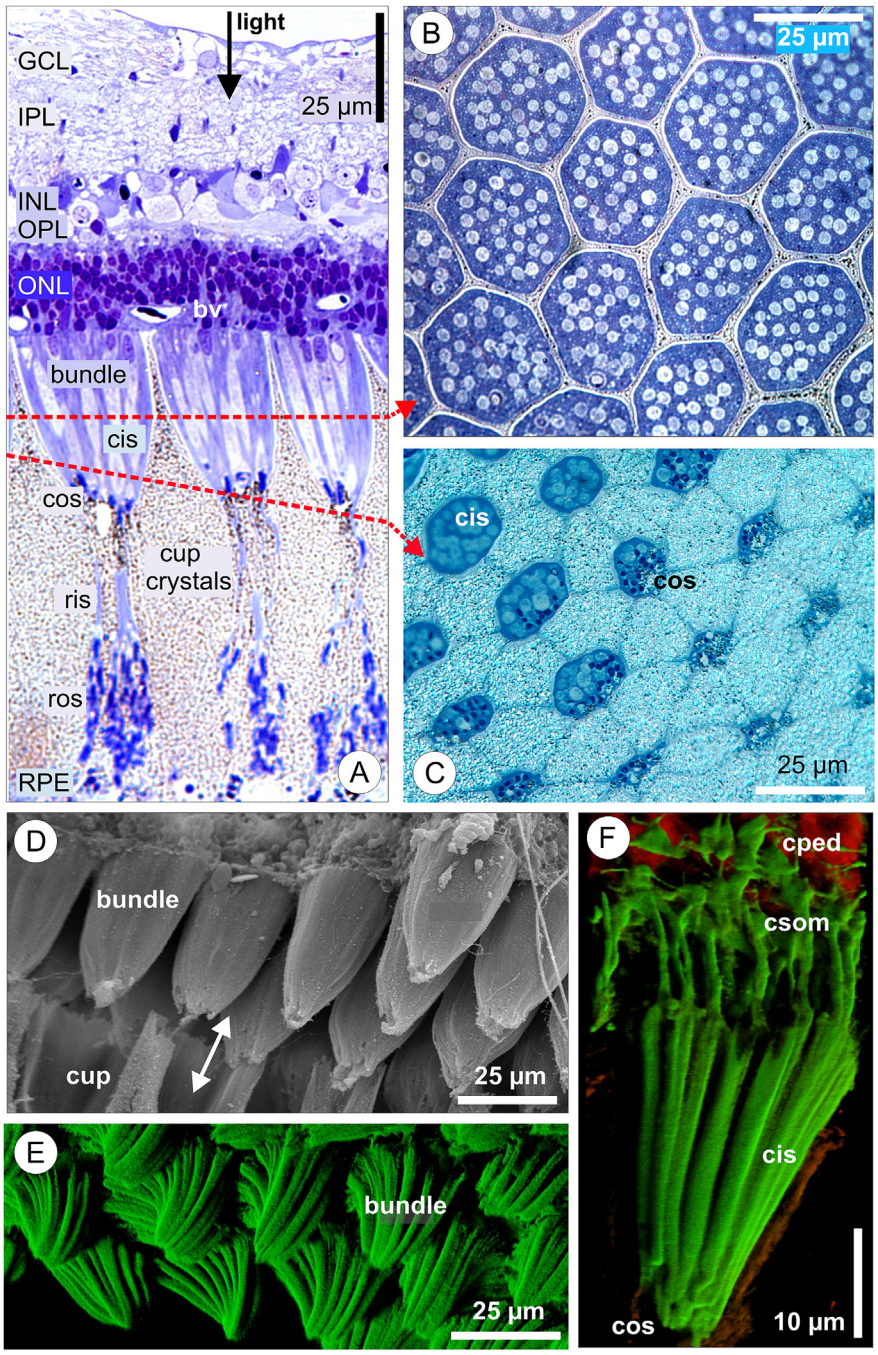

Fig. 9. Structure of the light-adapted *Gnathomus* retina. **A**, Radial semi-thin section through the central retina of an adult fish; the red dotted lines indicate the levels of the transversal sections shown in (B) and (C). B, Throughout most of their extension through the cup, the bundles consist of the (>20) thick cone inner segments (cis) and the much thinner processes of the rods (not visible at this magnification). **C**, near the 'bottom' of the cups, the cone outer segments (cos) are located. The rod inner (ris) and outer segments (ros) are situated – in respect to incoming light – behind the bottom of the cups (see A). **D**–**F**, Three-dimensional views of the bundles. **D**, Scanning electron microscopy of a retinal piece where the bundles were artificially separated from the cups during freeze-drying (arrow). **E, F**, Confocal images of anti T7-labeled cone bundles (*green*). **E**, Array of several adjacent bundles. **F**, Higher magnification of a single bundle, showing also the somata (csom) and synaptic pedicles (cped) of the cones. GCL, ganglion cell layer; IPL, inner plexiform layer; INL, inner nuclear layer; OPL, outer plexiform layer, ONL, outer nuclear layer; RPE, retinal pigment epithelium; bv, blood vessel. (A, B, modified from Kreysing et al., 2012; D, courtesy of Johhans Kacza, Leipzig).

and driftwood), in holes in the embankment, or at sites of dense vegetation, always close to current (Moritz, 2010; Ogbeibu and Ezeunara, 2005; Tawari-Fufeyin and Ekaye, 2007). The turbidity of the water was found to be relative high, with turbidity values between 45 and 1670.5 FTU (=*Formazine Turbidity Units*; see Ogbeibu and Ezeunara, 2002).

Like most mormyrids *G. petersii* hides during the day, becomes active at dusk and stays so throughout the night (Moller et al., 1979; Okedi, 1965, 1968). It is a bottom feeder, searching for small insect larvae, mainly chironomids (Diptera), which are buried in the soil. *G. petersii* digs them out, using its movable chin appendix. This is also indicated by the large amount of sand and organic matter

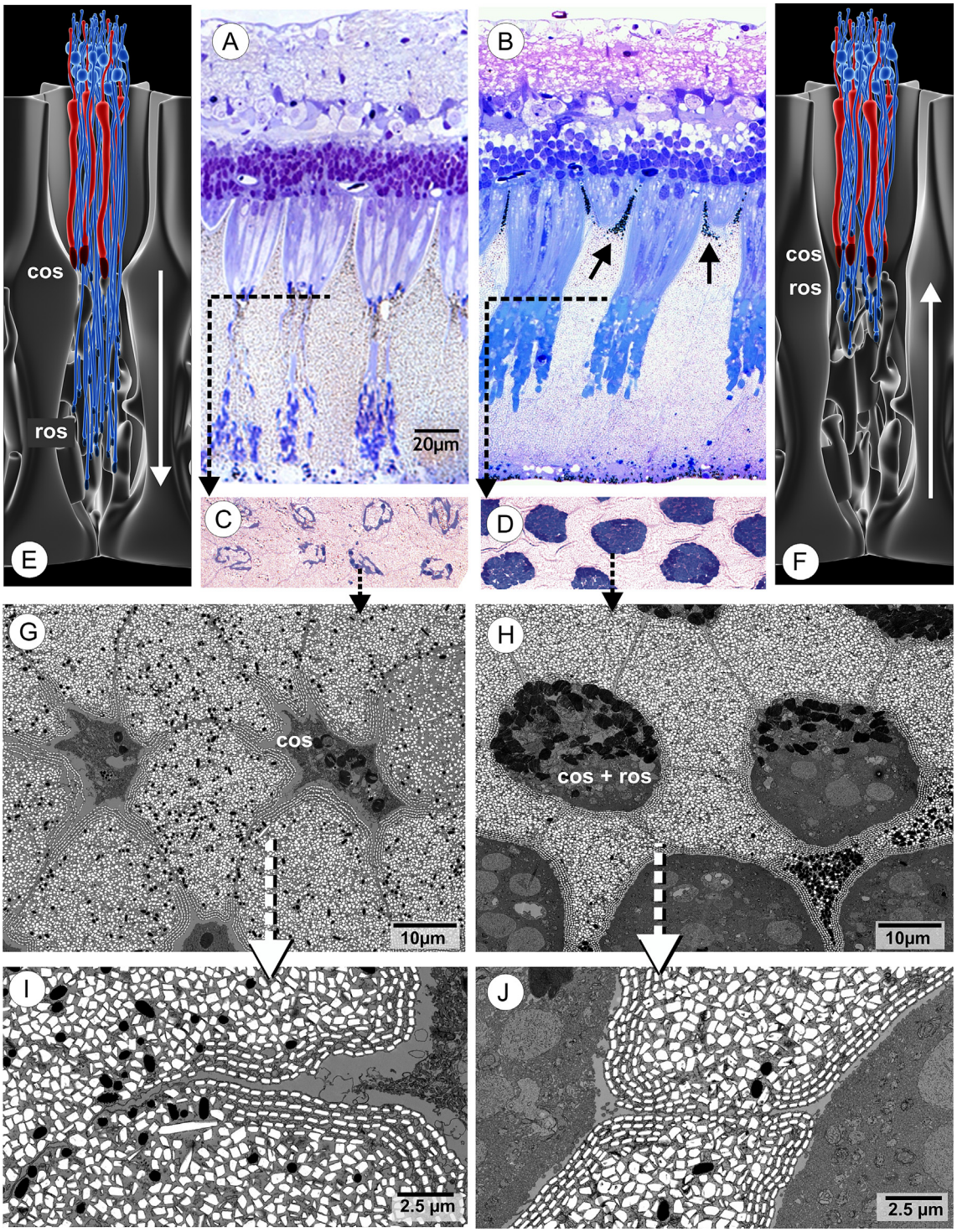

Fig. 10. Retinomotor activities of the *Gnathomus* retina related to light/dark adaptation. **A**–**D**, Semithin sections of light- (**A, C**) and dark-adapted retinae (**B, D**); the level of the tangential sections (**C, D**) is indicated by the dotted lines in the radial sections (**A, B**); it corresponds to the bottom ('bottleneck') of the cups in light-adapted retinae. In the light-adapted state (**A, C**) at this level only the cone outer segments (cos) are found whereas in the dark-adapted retina (**B, D**), the rod outer segments (ros) arrived at the same level. This is illustrated also in the schematic drawings (**E, F**); note that in order to give way for the accumulating rod outer segments, the cups widen at this level such they re-shape into cylinders (**B, D, F**). Note also that the pigment granules are more or less evenly distributed throughout the cores of the RPE cell processes in the light-adapted retina (**A**) but accumulate in their tips during dark-adaptation (**B, H**, arrows). **G-J,** Transmission electron micrographs of transversal sections through the bottom of the cups Level as in C, D). **G, I**, Light-adapted retina. The bottleneck is narrow and contains only cone outer segments. The multilayer of guanine platelets extends over a considerable distance into the clefts between adjacent RPE cells (**I**). **H, J**, Dark-adapted retina. The bottleneck is widened and contains both cone and rod outer segments. The multilayer of guanine platelets surrounds each bundle but extends only over a short distance into the clefts (**J**). The dotted arrows indicate at which level the tissue was cut to generate the picture below (A–D) or which part of (G,H) were magnified in (I, J), respectively.

found in their stomachs (Nwani et al., 2011). For detecting its prey on the ground, the active electric sense (active electrolocation) plays a dominant role, accompanied by the chemical senses and perhaps the mechanosensory lateral line system (Von der Emde and Bleckmann, 1998). Because they can perceive the capacitive properties of chironomid larvae, which distinguish living objects from the inanimate substrate they live in, the fish have evolved a special sensory sub-modality for prey detection (Von der Emde, 1993). The presence of light does not improve prey detection, suggesting that vision is not used during prey search. The prey items are rather small and thus probably not visually detectable by the fish, since *G. petersii* cannot see objects spanning less than about three degrees of visual angle (Schuster and Amtsfeld, 2002; Landsberger et al., 2008; Kreysing et al., 2012).

Generally, the dominant sense for object detection and identification in *G. petersii* is the active electric sense. It is very difficult to train the fish to react to the presence of an object that they only can see but not electrolocate (Schuster and Amtsfeld, 2002; Landsberger et al., 2008). In contrast, several studies have shown that *G. petersii* can quickly and easily learn to discriminate electrically between two objects differing in shape, size, material composition, or distance (reviewed by von der Emde et a., 2010; Von der Emde and Fetz, 2007). These studies also showed that the fish do not use vision to discriminate between stationary objects (even large objects of several centimeters size). Noteworthy, active electrolocation is a near-field sense. Depending on their sizes, objects are detected up to a distance of about 15 cm, i.e. about one fish length. Object identification is even restricted to a distance of 4–5 cm (Fechler et al., 2012). In summary, *G. petersii* does not use vision but its active electric sense for finding prey and to inspect stationary objects such as landmarks even when light is present. The visual sense thus must have a different function in the life of *G. petersii* (see Section 6).

Obviously, the visual sense of the fish is challenged by difficult light conditions. In the habitat of *G. petersii*, visual contrast will not only be affected by scattering but also by absorption. In this case a "veil", resulting from the scattering of light *into* the line of sight between object and fish (Fig. 7B), adds parasitic contributions to the relevant signal, which in turn reduces the visual contrast. Because in absorbing media intensity decreases exponentially with distance, the intensity ratio of light rays having traveled different distances changes with the absorption coefficient. This means that the impact of scattering on contrast attenuation increases with increasing absorption, because the ubiquitous "veil" (obscuring the signal) must travel a smaller distance to the eye than the relevant signal (Fig. 7B). Considering that the absorption of light in Gnathonemus' habitat is dominated by dissolved organic matter (Moller et al., 1979), which absorbs strongest in the blue and green, the importance of scattering and its wavelength dependence is only further emphasized, and the red part of the spectrum dominates (Fig. 7D).

This is in contrast to deep-sea water (Fig. 7E) where the overlaying water layers have absorbed most of the incident light except for the short-wavelength (blue) part of the spectrum (Fig. 7F; *black line*); moreover, most of the bioluminescence provided by deep-sea organisms is also in the blue part of the spectrum (Fig. 7F, *red line*). Accordingly, the cones reported to occur in some deep-sea fish retinae (e.g., Frederiksen, 1976) (Fig. 4E and F) can be beneficial for the fish if expressing blue-sensitive photopigments (Fig. 7F, spectrum of SWS cones).

4.2. A peculiar eye with 'spectacles' and retinal blood supply

If compared to other fishes, the eye and the retina of *Gnathonemus* show several pecularities of which are not all related to the specialized demands of vision in its habitat (Fig. 8). First, its eye is covered by a 'spectacle'. Spectacles or goggles are tissue layers covering the eyeball proper with its CNS-derived three main layers, i.e, sclera (dura mater), choroid (arachnoid) and retina (neuroepithelium). Their main function is to protect the eye from the surrounding media, such as water or air. Depending on whether or not the spectacle is fused with the transparent part of the sclera, i. e. the cornea, primary (i.e., fused) and secondary (separated) spectacles are distinguished. A tertiary spectacle represents a variation of the secondary type where the ocular bulb is covered by transparent lids that are joined to the eye by a conjunctival epithelium.

In *Gnathonemus* the eye is covered by unusually thick dermal layers that are mechanically and electrically remarkably resistant; incisions are difficult to make, and the electroretinogram can only be recorded when the electrodes are inserted into the eye proper, bypassing the spectacle. The native thickness of this skin is about 0.3 mm; it is composed of several layers, involving an outer epithelial epidermis with several sublayers and cell types, and a dense collagenous dermis on the inside, also with a complex substructure (see Fig. 8A). After fixation and thin sectioning of the eyes, a large gap between the inside of the spectacle and the cornea becomes evident (Fig. 8A, C), suggesting the presence of a tertiary spectacle as demonstrated in *Engraulis* sp. by Hein (1913). However, there is no epithelial lining of the putative anterior chamber in *Gnathonemus*, and in the unfixed frozen material the dura-equivalent cornea is tightly apposed to the dermal spectacle (Fig. 8B) suggesting that this space is artificial. It is tempting to speculate that the – electrically isolating – spectacle is necessary to protect the retinal information processing from disturbances caused by the electric activity of the fish.

The shape of the eye (as well as that of the lens) is almost spheroid (Fig. 8B). The maximum angular resolution to be obtained by a spherical eye can roughly be calculated as follows :

$$2 \times \text{spacing of photoreceptor units/focal length}$$

where the factor of 2 takes into account that the finest resolvable grating must be supported by at least two receptor units per period (cf. Land and Nilsson, 2002). Assuming that the main refractive power in the fish eye is contributed by the lens and that the eye is emmetropic, the focal length of the eye can easily be measured; it is about 2–3 mm, depending on the size of the fish. If the maximum resolution is restricted by the size of a cup (which is around 50 μm in diameter) this gives rise to maximum visual resolution of

$$2 \times 0.050 \text{ mm}/2.3 \text{ mm} = 0.0038 \text{ radians} = \underline{2.5 \text{ degrees}},$$

which indeed is very close to the actual visual cut-off of *Gnathonemus pertersii* (about 3 degrees: Fig. 18A; *cf.* also Kreysing et al., 2012). The macro-receptor organization can thus indeed explain the observed spatial frequency filtering (cf. section 6.2) to a very large extent. For comparison, the goldfish (that has no grouped retina) is known to visually resolve details at visual angles more than 15 times smaller (409 cycles per radian, corresponding to 0.14 degrees) (cf. Land and Nilsson, 2002).

Noteworthy, the bundles are not all directed toward the center of the eye but become more and more obliquely oriented to the retinal surface if more peripheral areas are studied (Fig. 8D–F). Very probably, this orientation toward the center of the pupil is aimed at increasing photon capture (Laties and Enoch, 1971). It appears to be general feature of vertebrate eyes, even if no macroreceptors occur in the retina (Enoch, 1980).

Finally, the presence of intraretinal blood vessels should be emphasized (Fig. 8G–L). It had already been noted by the first observers of Mormyrid retinae (Franz, 1921; McEwan, 1938) and

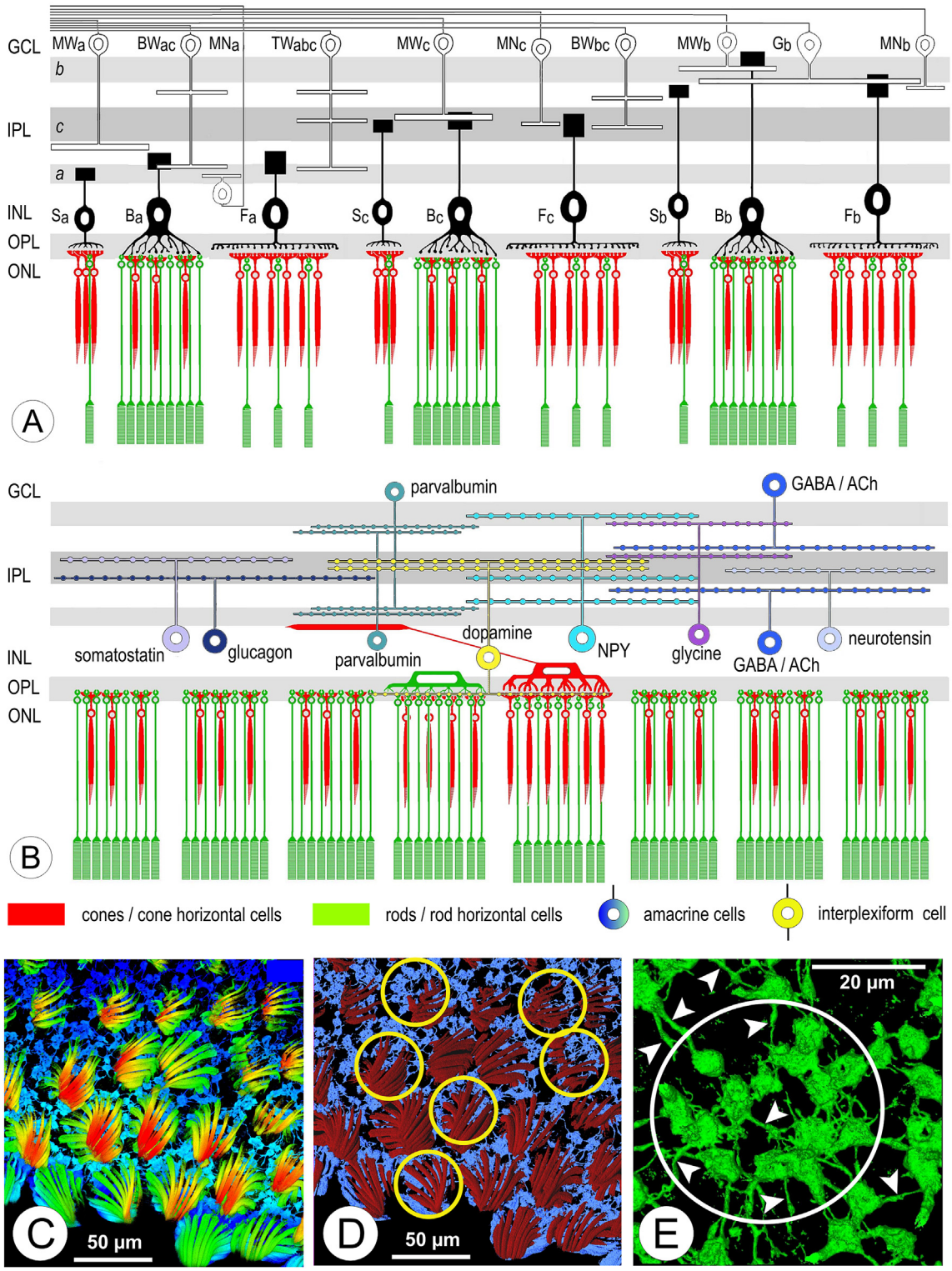

Fig. 11. Neuronal cell types and circuits of the *Gnathomus* retina. **A, B,** Schematic representation of photoreceptors and neuronal cell types based on Golgi staining (bipolar and retinal ganglion cells) neurobiotin labeling (horizontal and retinal ganglion cells) and immunocytochemistry (amacrine cells). The relative contributions of rods (green) and cones (red) to the input of bipolar (BC) and horizontal cells (HC) are indicated and the size of HC and BC dendrites relative to the bundle diameter is also given. By contrast, it was not possible to scale the dendritic field size of amacrine cell processes and retinal ganglion cell (RGC) dendrites relative to 'bundle grain'. **A**, Nine types of bipolar cells (solid black) were identified, flat (F), bushy (B) and small (S) cells extend their axons to sublaminae *a, b* and *c* of the inner plexiform layer (IPL). Ten types of RGCs (outlined in black) have three differendet dendritic field sizes; giant (G), widefield (W), and narrow (N); they are monostratified (M), bi-(B) or tri- (T) stratified. The subscript indicates the sublamina (*a, b, c*) in which their dendrites are localized (note that the schematic illustration of BC axon terminals as boxes is an oversimplification since the axon terminals are often branched or multilobed). **B**, Two types of HC were found; the green cell is a rod HC and linked only to rods; the red cell is a cone HC and gets input only from cones. Amacrine cells are shown in various hues of blue, indicating their specific morphology (stratification pattern) and their neurochemical signature as revealed by immunocytochemistry. A single type of interplexiform cells was identified by tyrosine hydroxylase immunocytochemistry (indicating the use of dopamine as transmitter; shown in yellow). **C-E**, Cone pedicles (specifically labeled by anti-T7; *blue* in C and D, *green* in E) are grouped according to the bundles, but are interconnected by axonal processes (*arrows* in E). **C**, Color-coded merge of a

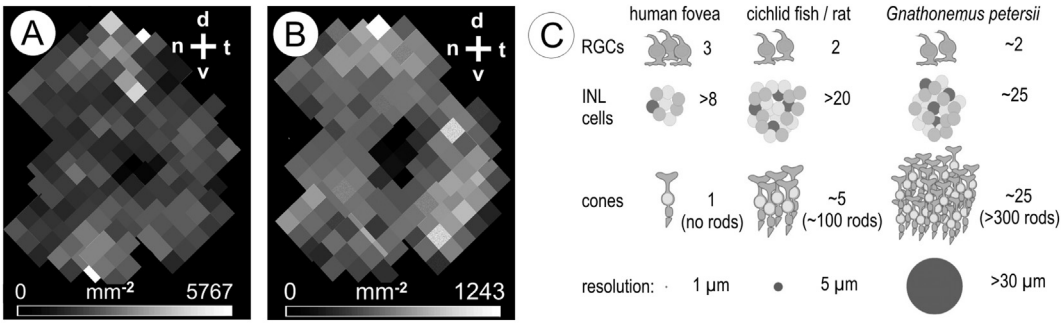

Fig. 12. Convergence in the *Gnathomus* retina. **A, B,** Local densities (indicated by the gray scales, in mm^{-2}) of retinal ganglion cells (RGCs; **A**) and photoreceptor bundles (**B**). **C**, Schematic comparison of neuronal circuits and resulting optical resolution (at the level of the retina) of the *Gnathonemus* retina with that of other vertebrates. Whereas the human foveola achieves a resolution of 1 µm when the information of one cone is transmitted to about 8 cells of the inner nuclear layer (INL cells) and about 3 RGCs, the retina of Gnathonemus represents the other end of the scale, with a resolution of some 30 µm, provided by about 25 cones for about 2 RGCs; other vertebrate retinae are in between these extremes. d, dorsal, t, temporal, v, ventral, n, nasal regions of retinal wholemounts.

was also found in the retina of the eel (Virchow, 1882; Michaelson, 1954). This is noteworthy since with these exceptions, the retinal tissue of fishes is devoid of blood vessels, and is nourished by the choroid (and often by blood vessels at the vitread retinal surface: Michaelson, 1954). In *Gnathonemus petersii*, three retinal layers/networks of capillaries can be demonstrated (in the ganglion cell and inner nuclear layers, and close to the external limiting membrane where they form 'rings' around the bundles: Fig. 8G–L). It appears reasonable to speculate that these intraretinal blood vessels are required to feed the retina, including the photoreceptor cells, because the very large and complex RPE cells constitute an obstacle against oxygen diffusion from the choroid. In the case of the eel, intraretinal blood vessels are required since a choroid is missing (Michaelson, 1954).

4.3. Structure of the light- and dark-adapted retina

Noteworthy, most of the data shown and discussed before were obtained from the light-adapted retina. Its structure is summarized in Fig. 9. Note that the diameters of the bundles may vary among individual fish, and even within a given retina, from about 30 to 50 µm.

However, similar to related fish species (Moore, 1944; Wagner and Ali, 1978; Awaiwanont et al., 2001; Nag, 2004; Taylor and Grace, 2005) the retina of *Gnathonemus* shows illumination-dependent retinomotor activity which considerably changes the structure of the outer retinal layers (Fig. 10). During dark adaptation at night, the cup widens at its bottom (such that the 'bottleneck' disappears) and assumes the shape of a cylinder. Concomitantly, the processes and inner segments of the rods shorten and thus their outer segments are drawn toward the incoming light, up to the same level as the cone inner segments (which fail to move significantly) (Fig. 10E, F). Similar retinomotor activities are long known to occur in fish retinae; in many cases, the cones undergo a counter-movement to the rods (Garten, 1907). Apparently, this re-arrangement of the light-sensitive elements allows for the most direct access of light to those receptors, which are responsible for light perception under the changing conditions of illumination, *viz.* the cones at daylight and the rods at night. Noteworthy, in *Gnathonemus* as well as in *Hiodon* (Wagner and Ali, 1978), the cone outer segments remain in a light-exposed position even after dark-adaptation, whereas the rods become effectively 'shielded' from light during daytime (cf. also sections 4.6, 5.1, and 6).

While the re-location of the photoreceptor outer segments can be explained by contractile processes in their myoid (Burnside and Basinger, 1983; Dearry and Burnside, 1984; Burnside et al., 1993) the light-adaptive changes in the RPE cells are less easily understood. In many teleosts, dark adaptation leads to an aggregation of the pigment granules in the sclerad portion of the cells (which is the far side from incoming light); this redistribution of organelles seems to be controlled by similar mechanisms as the mechanical responses of the photoreceptor cells (Burnside and Basinger, 1983; Dearry and Burnside, 1984). By contrast, in the dark-adapted *Gnathonemus* retina the pigment granules aggregate in the tips of the RPE cell processes which are directed toward the incident light (Fig. 10B, arrows). Moreover, whereas in 'conventional' RPE cells the movement of organelles through the cytoplasm should meet rather few obstacles, the large RPE cells of *Gnathonemus* are tightly packed with guanine crystallites (Figs. 4C and D, 10I and J).

Probably, these crystallites – together with the little cytoplasm surrounding them – constitute a non-compressible but highly viscous emulsion, filling the available space between the walls of the adjacent RPE cells outside, and the photoreceptor bundles inside the cup. When, during dark adaptation, the rod outer segments are retracted toward the level of the former 'bottleneck', the crystallite emulsion is pushed away (giving space for the photoreceptors, and allowing the widening of the cup bottom) into the more sclerad part of the RPE cell (which is no longer compressed by the rod outer segments). During light adaptation, the crystallite emulsion then moves back. By contrast, the multilayer of guanine platelets at the 'inner wall' of the cup should have a constant thickness, length, and width. Thus, it completely surrounds the large circumference of the 'opened' bottlenecks in the dark-adapted retina (Fig. 10H and J), but when the bottleneck is narrowed during light adaptation, the now-dispensable parts of the multilayer extend far into the clefts between adjacent RPE cells (Fig. 10G and I).

4.4. Retinal cell types: qualitative and quantitative data

Generally, retinal neurons transform the intensity-dependent graded (analog) input signals of the photoreceptors into the action potential (digitally)-coded, complex output signals of ganglion cells that convey information about contrast, movement, or object

stack of confocal images through the outer layers of the retina (from *red*, level of cone outer/inner segments, to *blue*, level of cone pedicles); **D**, merge of the levels showing the cone outer/inner segments (red) and the cone pedicles (blue). Some groups of pedicles are encircled. **E**, Higher magnification of a group of cone pedicles, emphasizing the connective axonal processes (arrows). GCL, ganglion cell layer; OPL, outer plexiform layer, ONL, outer nuclear layer.

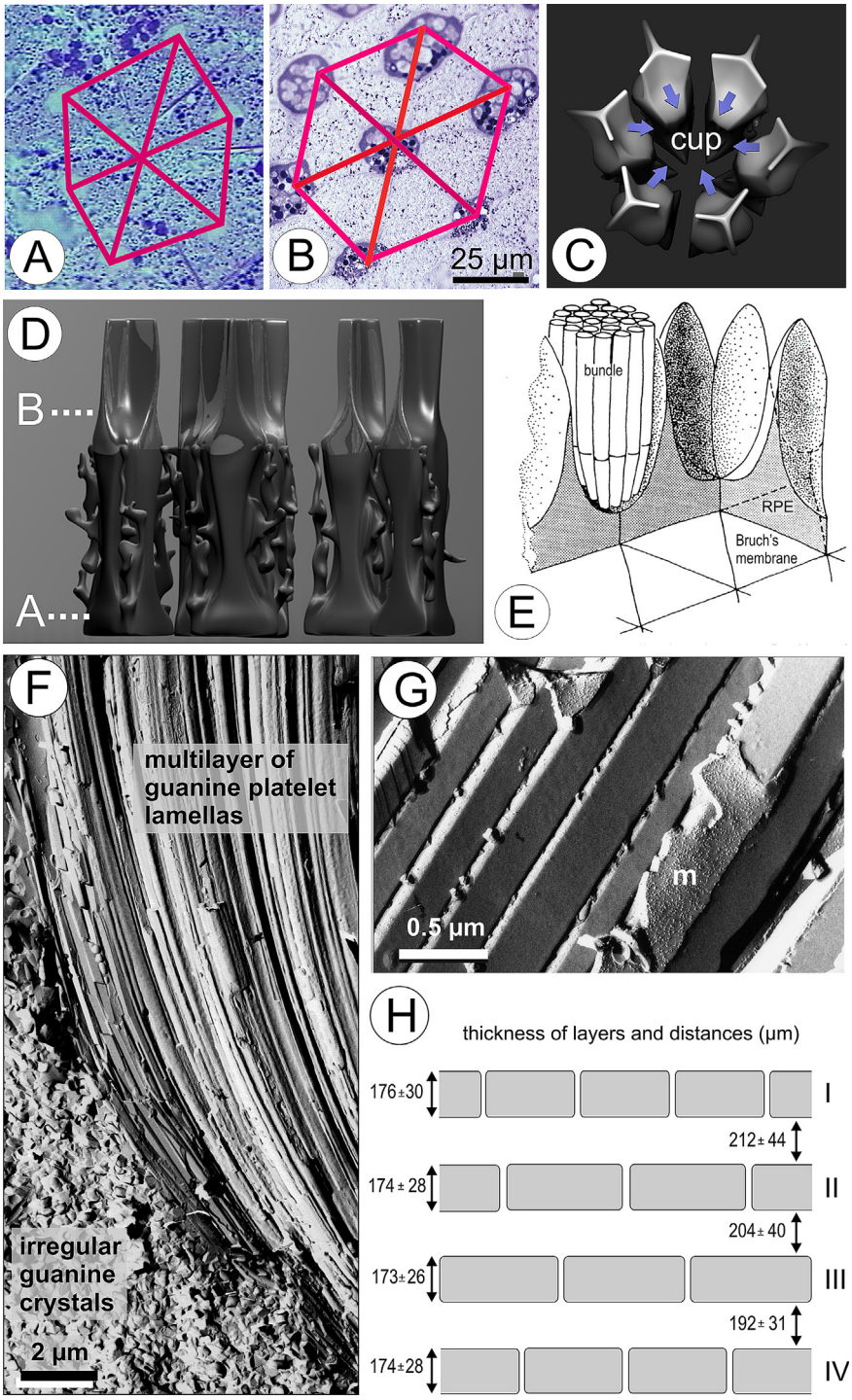

Fig. 13. Organization of the tapetum/RPE in *Gnathonemus petersii*. **A, B**, Transversal semithin-sections of a retinal wholemount at the levels of the RPE cell nuclei (**A**) and close to the bottom of the tapetal cups (**B**); the hexagonal arrangement of the cells and their processes is indicated by the red lines. **C, D**, Artist's view of six RPE cells contributing to one cup; light-adapted conditions. **C**, Each of the large cells extends from the soma (*bottom*, level of section A) to the aperture of the cup, close to the outer limiting membrane (*top*). The 'upper' (retina-facing) parts of the processes of six adjacent cells together form a smooth, light-reflecting cup (**D**). Below the bottom of the cup (close to the level of section B) the RPE cell processes form less regularly shaped sheaths around the bundles of rod inner and outer segments. **E,** Schematic drawing of the bundle structure in the main and accessory retina of *Scopelarchus michaelsarsi*, for *comparison (from Locket, 1971)*. **F, G**, Electron microscopy of freeze-fracture replicas of the wall of a cup (close to the level of section B). The surface of the cups is constituted by three to four layers of venetian blind-like guanine lamellae which appear as platelets in transversal sections (cf. Fig. 4C, D). The main part ('inner core') of each RPE cell process is filled by less-regularly shaped crystals, down to the level of the cell soma. The lamellae are only present between the aperture and the bottom of the cup proper. m, cell membrane overlaying one of the lamellae. **H**, Average thickness of the lamellae, and distances between them in the four layers (I-IV). Noteworthy, the very same dimensions were found in dark-adapted retinae. (F–H, modified from Kreysing et al., 2012).

size to the higher centers of the brain (for a recent review, see Masland, 2012). In the outer plexiform layer (OPL in Fig. 11), rods and cones are linked to each other by gap junctions, and make unconventional ('ribbon') chemical synapses to horizontal and bipolar cells. Modulatory input to this layer is provided by interplexiform cells, a dopaminergic subtype which is present in *Gnathonemus* and other teleosts. The inner plexiform layer (IPL in Fig. 11) is considerably wider than the OPL, and contains

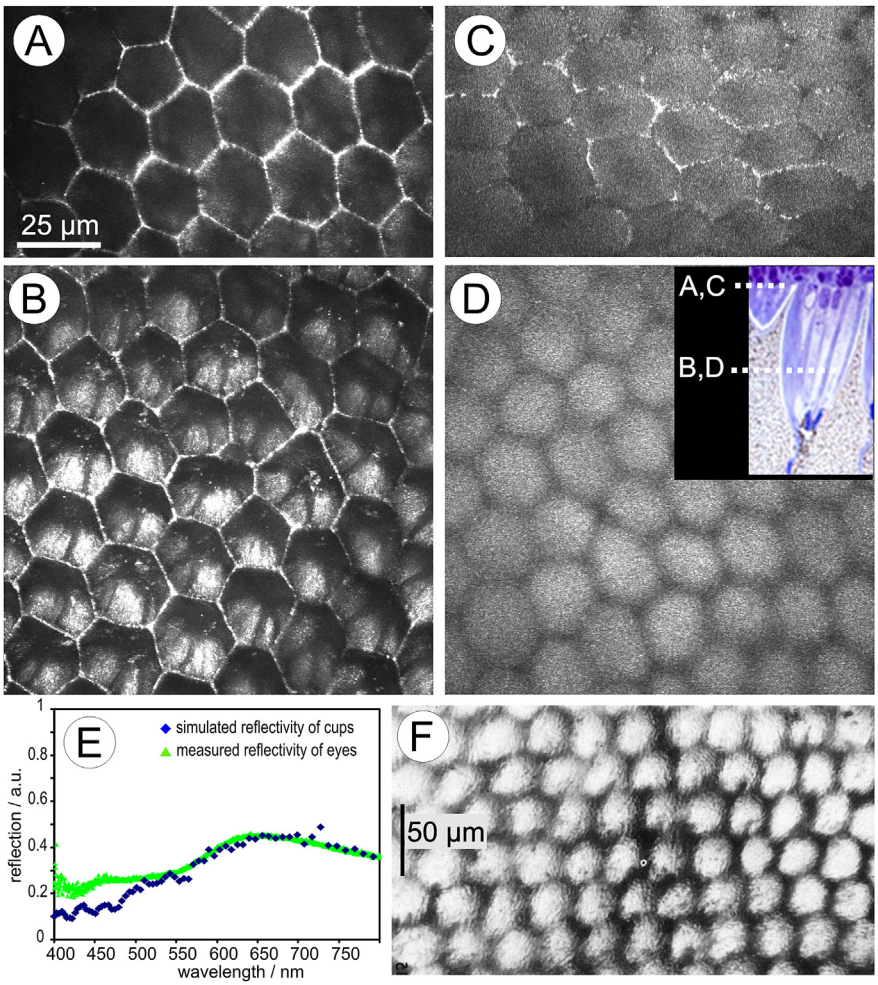

Fig. 14. **A**–**E**, Light reflection by the tapetal cups of *Gnathonemus petersii*. A–D, Confocal microscopy of native, unfixed retinal wholemounts in the reflection mode of the laser scanning microscope. **A, B**, In the light-adapted retina, strong light reflection is visible both at the upper margin (aperture) of the cups (**A**) and at their inner surface (**B**). **C, D**, In the dark-adapted state, light reflection at the aperture is maintained (**C**) but is no longer visible at the inner surface (**D**); rather, the inner rod and cone segments of the bundles now display a moderate backscattering of light. The inset in **D** shows the focus levels of **A**–**D**. **E**, Measured (*triangles*) and simulated (*squares*; cf. Fig. 15) reflection of light from a native retinal wholemount; longer wavelength are reflected better than short ones. **F**, Light transmission through a native, dark-adapted retina of *Hiodon tergisus*, after removal of the RPE. A retinal wholemount was viewed from the sclerad side and illuminated from the vitread side. Note that the inner segments (ellipsoids) of the bundled photoreceptor cells display a light-guiding effect whereas less light passes between the bundles; modified from Wagner and Ali (1978). (B and E, modified from Kreysing et al., 2012).

presynaptic bipolar cell terminals that project onto retinal ganglion cell (RGC) dendrites; furthermore, amacrine cells also receive input from bipolar cells and modulate the RGC receptive field signals in multiple ways.

As in other vertebrate retinae, the IPL is subdivided into several structural and functional sublaminae (Fig. 11A and B). The band adjacent to the inner nuclear layer mediates light-Off signals and is termed sublamina *a* (Famiglietti and Kolb, 1976); by contrast, the neuropil next to the ganglion cell layer mediates signals of the light-On pathway and is termed sublamina *b*.

The intermediate 3–4 µm wide strip contains RGC dendrites producing On–Off responses; morphologically it is characterized by a particularly high volume density of bipolar cell terminals (Landsberger et al., 2008). It is flanked on both sides by GABA/ACh – containing starburst amacrine cells (Fig. 11B, *right side*).

Nine types of bipolar cells (BCs) were identified in *Gnathonemus petersii* (Fig. 11A; Wagner, 2007), (i) small BCs with dendritic field diameters between 20 and 30 µm (i.e., slightly narrower than the bundle size); they receive input predominantly by cones; (ii) BCs with bushy dendrites roughly matching the bundle diameter (>30 µm); they receive strongly rod-dominated input; and (iii) flat BCs with dendrites that have a comb-like appearance and are considerably wider than a photoreceptor bundle; they are contacted by some rods but mostly by cones. As the pedicles of the cones within a bundle appear to be grouped in the outer plexiform layer and leave some space to the neighboring group (Fig. 11C–E), the dendritic field size of the small bipolar cells may match the size of one such group; thus, every small BC may collect the information of the cones (and some rods) of a bundle. Immunocytochemistry against protein kinase C reveals a population of BCs that closely resembles the B_b cells (i.e., one type of bushy cells, Fig. 11A). The spatial density of these cells is about 1.6 times higher than that of the photoreceptor bundles. Each of the three basic BC types has three sub-types sending their axon terminals to each of the three IPL sublaminae, making sure that in each sublamina the three different information pathways are represented in parallel. Although all BC types receive input from rods and cones, the following three distinct information pathways can be identified, (i) a signal transferring information dominantly from the cones of a bundle (small BCs); (ii) a rod dominated signal roughly at 'bundle grain' resolution (probably, slightly overlapping with signals from neighboring bundles), and (iii) a mixed, but cone-dominated signal involving information from several bundles. In comparison, the cohort of nine BC types in *Gnathonemus* is much less differentiated

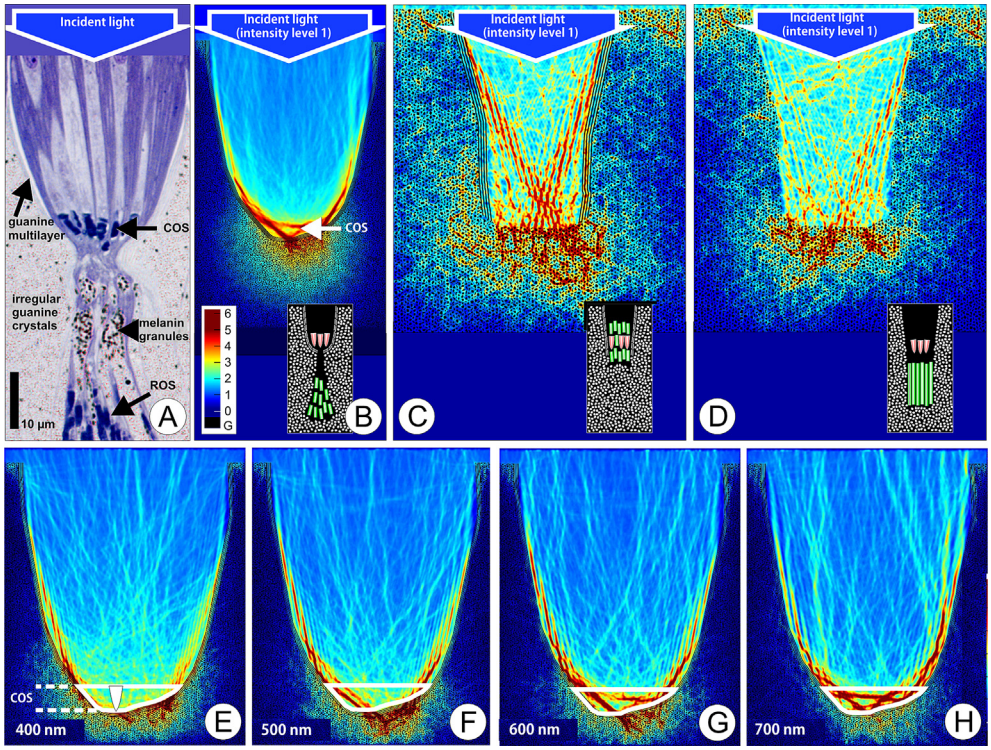

Fig. 15. Light collection by the tapetal cups of *Gnathonemus petersii*. **A**–**B**, Light-adapted retina (cf. Figs. 8, 9 and 15). **A**, Semithin section through a bundle and its tapetal sheath, indicating the structures for which the simulation (**B**) was made. **B**, Simulation of the light intensity distribution in a cup for an incident plane wave of broad spectral range (525–725 nm). The COS receive up to 500% of the incident light intensity whereas the ROS receive ≤ 20%. Color scale shows local gain; G = guanine. **C**–**D**, Dark-adapted retina (cf. Fig. 14B, D, F). **C**, Simulation as in (B), but for a dark-adapted cup widened at its bottom (i. e., without the 'bottleneck'). **D**, Structure as in (B), for a cup but without regularly spaced guanine multilayer (i. e., with the irregular crystals only); noteworthy, a similar light distribution can be assumed for the 'simple duplex cup' (inset). **E**–**H**, Simulations as in (B) but for monochromatic illumination at (E) 400 nm, (F) 500 nm, (G) 600 nm, and (H) 700 nm. The images clearly show an increased intensity of light for longer wavelengths, as indicated by increasing deep-red color coding of light intensities (cf. Figs. 7D and 14E). The area surrounded by a white line indicates the location of the cone outer segments (COS) and was used to integrate the average gain at the level of the COS. The insets in **B**–**D** indicate for which type of cup/light adaptation state a given simulation is representative (cf. Fig. 5). (A, B, and E–H modified from Kreysing et al., 2012).

than the 18 BC types in zebrafish (Connaughton et al., 2004). While the dendrites and their rod/cone input are similar in both species, the complex organization of its inner plexiform layer (involving a higher number of sublaminae) may account for the higher number of BC types in the tetrachromatic zebrafish.

Among the horizontal cells (HCs) two cell types were distinguished that conform to the general structure and function of HCs in teleosts since, contrary to BCs, they are strictly either rod- or cone-specific in their input (Fig. 11B, Landsberger et al., 2008). The dendritic fields of both the cone and the rod HCs roughly match the diameter of photoreceptor bundles. Cone HCs have a thin axon that runs within the INL and forms a 'nematode-like' swelling at the outer margin of the IPL, where it may contact perikarya of amacrine cells.

Among all retinal neurons, amacrine cells (ACs) display the greatest morphological and neurochemical diversity, and even though the inner retina of *G. petersii* is not as complex as in other, more visually oriented teleosts, this applies also to this retina. The present summary is based on the stratification pattern of AC processes throughout the sublaminae of the IPL (Fig. 11B). In accordance with their modulatory function, the area covered by the AC processes far exceeds the 'bundle grain' and may cover as many as about a dozen bundles. Each sublamina contains a characteristic 'cocktail' of neuroactive substances, especially neuropeptides. In sublamina *a*, we found (i) monostratified processes of starburst ACs in which GABA and ACh are colocalised, (ii) parvalbumin-immunoreactive (-ir) bistratified, and (iii) NPY-ir trilaminar ACs. Sublamina *b* contains the 'mirror-image' population of (i) starburst cells and (ii) parvalbumin-ir cells, i.e. with their perikarya in the ganglion cell layer, (iii) processes of the NPY-ir cells, and in addition (iv) glycinergic fibers of a bistratified AC. This shows that these two sublaminae are similar with regard to their neurochemical 'signature'. By contrast, sublamina *c* contains the greatest variety of AC processes, involving monostratified (i) neurotensin-ir, (ii) glucagon-ir, and (iii) somatostain-ir ACs, as well as processes of (iv) the bistratified glycinergic and (v) tristratified NPY cells. Furthermore, sublamina *c* contains a dense fiber plexus of dopaminergic interplexiform cells.

Like those of the ACs, RGC dendrites have diverse and specific branching patterns. For classifying GC subtypes in *G. petersii*, however, only the stratification pattern throughout the IPL sublaminae was considered, in addition to the diameter of dendritic field. Ten morphological subtypes were identified on this basis (Landsberger et al., 2008; Pusch et al., 2013). There was a single giant (G) monostratified RGC type with a dendritic field size exceeding 300 µm; it is localized in sublamina *b*. Other monostratified RGCs have dendritic fields sized between about 100 and 300 µm, termed widefield (W), and between 50 and100 µm, termed narrow (N). Each of these RGC types is present in each of the three sublaminae. Whilst, as a rule, RGC somata are found in the GCL, most somata of the N_a cells are localized in the INL. Furthermore, there are two types of widefield bistratified (BW) RGCs one with dendrites in sublaminae *a* and *b*, and the second one in sublaminae *b* and *c*, as well as a single type of trilaminar widefield (TW) RGC with dendrites in all three sublamiae.

Summarizing the data, the neuronal cell types and circuits of the *Gnathonemus* retina are basically similar to those of other fish retinae but there are peculiarities. First, the total width of the IPL is rather thin (15–18 µm; *cf.* Fig. 9A), similar to catfish and deep-sea fish that have either pure rod retinae, or typically possess only a

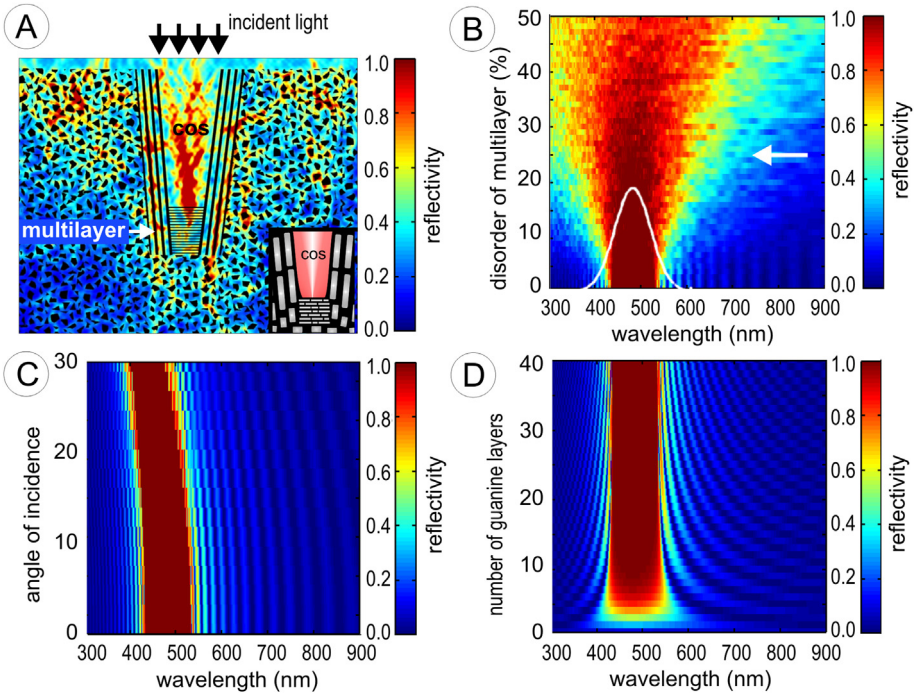

Fig. 16. Light intensification of the tapetal 'single-outer-segment'cups of deep-sea fish (cf. Fig. 5 and inset in A); simulations based upon an arrangement of 30 layers of 65 nm guanine platelets and 90 nm spacing. **A**, Simulation of the light intensity distribution in a single-outer-segment cup for an incident plane wave at 480 nm; note that the cone outer segment (COS) receives high light intensities throughout its length. **B**, Wavelength-dependence of the reflectivity by the crystaline multilayer at the bottom of the cup. Assuming an 'ideal' regular arrangement of the platelets, the reflectivity shows a narrow spectral range (see also C, D). Introducing some variability of the platelet thickness and spacing the reflection peak broadens with increasing degree of disorder of the multilayer. Noteworthy, this increases the overlap of the reflection peak and the absorption spectrum of a pigment with maximum absorption close to 480 nm (*white line*; *cf.* Table 2 and Fig. 7G). In the spectral range of the photopigment, a 30 layer mirror rises in effective reflectivity from 85% to 95% when the disorder increases from 0 to 20% standard deviation (*white arrow*). **C**–**D**, Boundary matching calculations for a regular arrangement of the multilayer. **C**, Maximum reflectivity occurs in the wavelength range between 400 and 500 nm, for angles of incidence up to 20 degees. **D**, When the number of layers is reduced in the simulation, the wavelength selectivity and the magnitude of the reflectivity become less sharp; The reason for multilayers with more than 10 periods to be found in fish is likely to be an enhanced performance in the presence of spatial variations..

single type of cone. In tri- or tetrachromatic fish such as goldfish, the IPL is generally more than twice as wide. It is intriguing to note the case of the mesopelagic pearleye (*Scopelarchus michaelsarsi*) which contains different retinal regions in its eyes, among them an area with grouped rods and an area with 'conventional', ungrouped rods (Locket, 1977; Collin et al., 1998). Here, the IPL associated with the grouped rods is markedly narrower than the IPL in the ungrouped region, suggesting that information processing in the grouped retina is less complex than elsewhere. This, together with the fit of the dendritic field sizes even of the 'small' bipolar cells with that of the bundles, argues in favor of the concept of photoreceptor bundles acting as functional units.

Furthermore, the retina of *Gnathonemus* appears to lack local specializations such as visual streak or area or a fovea centralis; backfilled RGCs and photoreceptor bundles in wholemount preparations roughly display a rather even and parallel topographic distribution across the retina (Fig. 12A and B). The average ratio of 2 RGCs per bundle involves an excessive convergence of the signals, as every bundle contains about 25 cones and several hundred rods (Fig. 12C). This supports the idea that the maximum resolution at the level of the retina corresponds to 30–50 μm (depending on the diameter of the cups), which is much more coarse than in the human fovea or even in 'conventional' fish retinae. Nonetheless, the presence of 10 types of RGCs suggests that like in other retinae, the visual stimuli are broken down into different parallel pathways. Fast and dynamic signals may be mediated by the giant monostratified and bistratified GCs, and the starburst amacrine cells may provide for direction/movement sensitivity (Vaney and Taylor, 2002; Taylor and Smith, 2012). Noteworthy, from the OPL on, the information provided by rods and cones may be pooled already at the bipolar cell level (Fig. 11A) such that color information is unlikely to be mediated to the brain (see section 6).

4.5. Structure and ultrastructure of the tapetum (retinal pigment epithelium)

In *Gnathonemus*, the RPE cells are hexagonally arranged (Fig. 13A, B, D); each six cells form a cup (and a more irregular-shaped sheath for the inner and outer segments of the rods) while every cell contributes to three cups/sheaths (Fig. 13D). This is similar to the cups in the retina of *Scopelarchus* (Fig. 13E) (Locket, 1971). The long, roughly columnar RPE cells of *Gnathonemus* enclose the photoreceptor bundles in two different manners.

In their 'upper', distal parts (which reach up to a level close to the outer limiting membrane of the retina proper) they form the cups, containing all the photoreceptor processes. At the bottom of each cup, the cone outer segments of one bundle are located (cf. Figs. 5, 9, and 10). Their proximal parts (between levels A and B in Fig. 13C), are less regularly shaped; they ensheath the inner and outer segments of the rods of the bundle. These proximal RPE cell processes extend several finger-like branches which constitute 'niches' around sub-groups of rod outer segments (cf. Fig. 10A, C). During dark adaptation, the distal RPE cell processes re-shape to form cylinders rather than cups (Fig. 10 B, D) but the basic subdivision into distal and proximal processes is retained. This applies especially to the structure of the guanine crystals within the RPE cell processes. The inner core of these processes is densely packed with irregular, polygonal crystals along their entire length from cell soma to near the aperture of the cups.

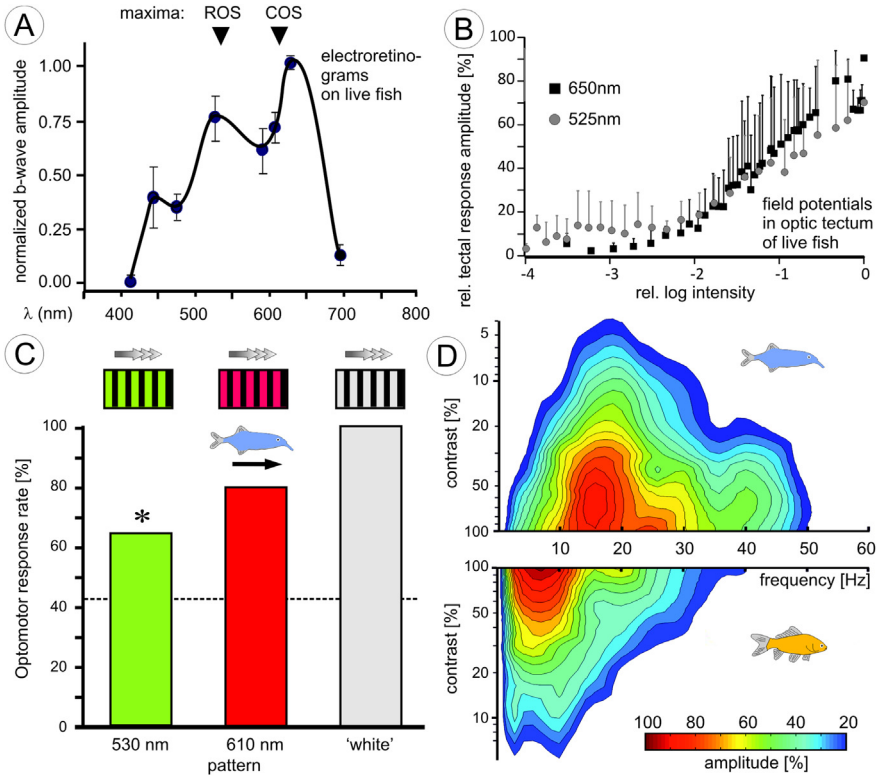

Fig. 17. Electrophysiological and behavioral consequences of rod and cone signal pooling in *Gnathonemus petersii*. **A**, Retinal action spectrum obtained from averaged electroretinograms of light-adapted fish; as indicated by the absorption maxima of isolated rod (ROS) and cone outer segments (COS) (cf. Fig. 7D), both types of photoreceptors contribute to the retinal response. **B**, Field potentials recorded in the optic tectum in response to green and red light flashes of different intensities show that the tectal response of the fish is fully matched in sensitivity at both wavelengths. **C**, The optomotor response rate of *Gnathonemus* was reduced when green stripes were presented rather than white ones ($p < 0.05$) (spectral and 'white' light intensities were equalized by neutral filters). However, green as well as red stripes reliably elicited responses. Dotted line: Normalized rate of false responses. **D**, Temporal resolution of *Gnathonemus petersii* compared to *Carassius auratus*. Electrophysiological measurements in the retina and the optic tectum (latter results shown here) of both fish show that *Gnathonemus petersii* can detect signals with higher temporal frequency and at lower contrast than *Carassius auratus*. (A-C, modified from Kreysing et al., 2012).

Additionally, the distal (but not the proximal) processes contain three to four regularly arranged layers of lamellar guanine platelets close to their bundle-facing surface (Fig. 13 E–G). Although the shape of the distal processes changes during dark adaptation, the arrangement of the lamellar crystals remains unchanged.

It has long been known that guanine crystals (particularly, if shaped as regular platelets) are well-suited as light-reflecting structures (Denton and Nicol, 1965). In fact, guanine has the highest refractive index (1.83) of all biological materials, and is used in the reflective tapetum of many fishes (Somiya, 1980) including those with grouped retinae (Table 2). The light reflection of native, isolated retinal wholemounts can be visualized (Fig. 14A–D) and measured (Fig. 14E). By this, the light-reflective properties of the cup walls can be nicely demonstrated in light-adapted retinae (Fig. 14A, B). Light reflection of the cup aperture is maintained in dark-adapted retina (Fig. 14C) but not longer demonstrable at the walls of the cup proper (Fig. 14D). Probably, it becomes then overlaid by the diffuse backscattering of the crowded photoreceptor cell processes (Fig. 14D). During light adaptation, i.e., when the cups are fully functional, it was found for *Gnathonemus petersii* that light reflection is stronger at longer wavelengths ('red') than in the short-wavelength range (Fig. 14E). It has also been shown in dark-adapted retinae of the related species, *Hiodon tergisus*, that the inner segments (ellipsoids) of the photoreceptor cells act as light-guiding structures (Fig. 14F) (Wagner and Ali, 1978).

Taken together, the data obtained on the light-adapted retina support the view of McEwan (1938) that "guanine would serve to throw back the light into the visual elements" – but only for the cones – as well as the suggestion of Moore (1944) that it provides "a shielding of the rod outer segments from bright light".

5. Tapetal cups as photonic crystal light collectors

To move beyond speculation about the function of the tapetal cups in the *Gnathonemus* retina, and to provide quantitative information, these days we can resort to directly simulating the interaction of light with these complex optical structures using numerical techniques – an option not available to McEwan and Moore more than 60 years ago (Kreysing et al., 2012). We will reiterate some of these recent results here and also try to apply similar simulation methods to other fish species with similar tapetal cups.

5.1. Comprehensive modeling for Gnathonemus petersii

The tapetal cup in *Gnathonemus petersii* displays an exquisite complexity with highly ordered and regularly spaced guanine crystal platelets lining its interior on a sub-wavelength scale and its overall roughly parabolic geometry on a scale 100 times above that. The maintenance of such structures surely bears a considerable metabolic cost, which begs the question of its functional optical advantage. While one can already infer the guanine multilayer, lining the cup, to act as a hot mirror for large angles of incidence from classical calculations, it is more difficult to estimate how much focusing power an imperfect parabolic mirror made of this material would have, and how much the light-sensitive outer segments,

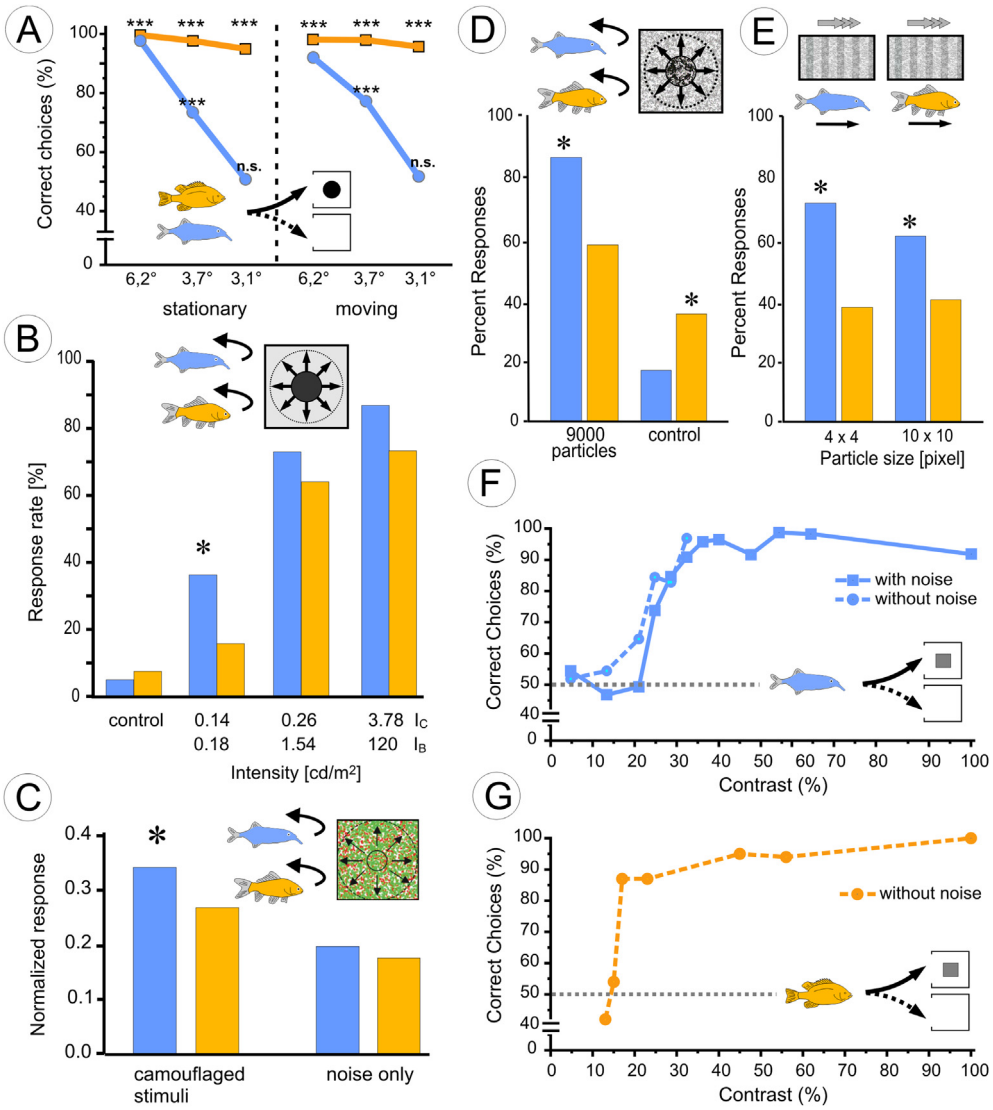

Fig. 18. Behavioral consequences of rod and cone signal pooling in the macroreceptors of *Gnathonemus petersii*. **A**, Spatial resolution is poor in *Gnathonemus* vision. Percentage of correct choices (to swim into a box with or into one without stimulus, see inset symbols) in response to stimuli of different size. Whereas *Lepomis* detect small stationary or moving stimuli (3.1° visual angle) as reliably as large ones, the correct choices of *Gnathonemus* fall down to chance level at these smaller stimuli, i.e. these small objects are no longer detected by the animal. **B**–**C**, *Gnathonemus* responds at low intensities and despite color-camouflage, **B**, Startle experiment with black circles expanding on a white background. The intensities of circles (I_C) and background (I_B) were varied. At low intensities, *Gnathonemus* (blue) performed better ($p < 0.05$) than *Carassius* (amber; $n = 5$ for both species). **C**, Startle experiment with color-pooling task. The expanding circle was dynamically defined by the random exchange of equiluminant red and green floating particles, with the particles inside the circle becoming stationary. *Gnathonemus* detected such color-camouflaged stimuli significantly better ($p < 0.05$) than *Carassius* ($n = 5$ for both species). The rate of false responses (right pair of columns) was not significantly different between species. Response percentages are relative to an expanding black circle (=1.0). **D-G**, *Gnathonemus* displays a high tolerance against spatial noise. **D**, Startle experiment with an expanding circle disguised by dynamic gray noise particles (9000 particles). Flight responses declined in both species (percentage relative to no noise), but *Gnathonemus* (blue) was less affected than *Carassius* (amber; $p < 0.05$) and produced less false responses with noise only (control) ($p < 0.05$). **E**, Percentage of optomotor responses to reversal of moving stripes relative to response rate without noise. When the stripes were obscured by dynamic white particles of varying size *Gnathonemus* performed significantly better than *Carassius* ($p < 0.05$). **F**, Contrast detection of *Gnathonemus* and **G**, *Lepomis* with and without added dynamic noise particles. Fish were trained to approach a black square on a bright background; the contrast of the square was reduced stepwise. The performance of *Gnathonemus* decreased only slightly when noise particles (black squares with a side length 2–8 mm, which corresponds to a visual angle size of 0.15°–0.6°; life time: 3 s; noise density 44%) were added (solid curve). Note that *Lepomis* refused to make any choices when images were overlaid by noise particles – even at 100% contrast. Modified from Kreysing et al. (2012).

located at the bottom of the cup, could benefit from it. This estimation of light intensity increase becomes even more complicated when trying to take into account the disordered phase of guanine crystallites surrounding the multilayer, (*cf.* Fig. 13F), as these by themselves have to be seen as a strongly back-scatting material with a transport mean free path length of only a few micrometers. In order to take into account both the relevant wave-optical effects such as interference and diffraction, as well as the global shape of the cup-like cavity, we modeled the entire system using the finite difference time domain method (FDTD), a numerical method for propagating electromagnetic waves on a grid with an arbitrary refractive index distribution. A particularly flexible set of algorithms, compatible with parallel computing, as required for the treatment of structures significantly bigger than the wavelength involved, is provided in the open source package MEEP (*ab-initio.mit.edu/wiki/index.php/Meep).* In addition to providing spatially resolved intensity distributions around or inside structures of interest in response to monochromatic light sources (of a single wavelength), FDTD also allows for the implementation of light pulses with finite spectral width (containing many wavelengths).

Using these FDTD simulations we provide several interesting insights into the functioning of tapetal cups. First, during light

Table 2
Summary of available data on visual pigments and tapetal crystals in fish species possessing a grouped retina. *Cursive* lettering indicates uncertain values (measured on printed images), question marks indicate that the λ_{max} values might not be measured on cones (or 'cone-like photoreceptors' of deep-sea fish); see text for details. The thickness of platelets (first value) and of the distances between them (second number), as well as the λ_{max} values, are given in nanometers. References are, 1. Somiya (1989); 2. Kreysing et al. (2012); 3. Nag (2004); 4. Best and Nicol (1979); 5. Braekevelt (1982); 6. Wagner and Ali (1978); 7. Zyznar et al. (1978); 8. Awaiwanont et al. (2001); 9. Kondrashev et al. (2012); 10. Novales Flamarique (2011); 11. O'Connel (1963); 12. Zyznar (1975); 13. Somiya (1980); 14. Locket (1971); 15. Locket (1977); 16. Partridge et al. (1992); 17. Pointer et al. (2007); 18. Munk (1977); 19. Munk (1966); 20. Douglas and Partridge (1997); 21. Douglas and Partridge (personal communication 2013); 22. Frederiksen (1976).

Genus	Species	Habitat	λ_{max} rods	λ_{max} cones	Crystals material	Rod-cup platelets	Cone-cup bottom platelets	Cone-cup lateral crystals	Ref.
Gnathonemus	petersii	Turbid	536	615	Guanine	175/210			1, 2
Marcusenius	longianalis	Turbid			Guanine				1
	isidori	Turbid			Guanine				1
Notopterus	notopterus	Turbid				*80/100*			(3)
Hiodon	alosoides	Turbid	535		Uric acid	*180/200*			4, 5, 6, 7
	tergesius	Turbid	535		Uric acid				6, 7
Engraulis	japonicus	Turbid	502	475 492 502	Guanine/ hypoxan-thine	*300/200 ?*		*180/150*	8, 9, 10
	mordax	Turbid			Guanine				11
Stizostedion	vitreum	(Turbid)			Pteridine				12
Polymixia	japonica	Dark			Guanine				13
	berndti	Dark			Guanine				13
Scopelarchus	güntheri	Dark			Guanine	*150/100*			14, 15
	sagax	Dark			Guanine				14
	michaelsarsi	Dark						*200*	
	analis	Dark	479	*505→ 444 ?*					16 + 17
Benthabella	infans	Dark	451		Guanine				15, 16
Scopelosaurus	lepidus	Dark				*160/100*	*60/50*	*200/200*	18
Ahliesaurus	berryi	Dark	487						19
Chlorophthal-mus	albatrossi	Dark			Guanine				13
	nigromarginatus	Dark			Guanine				13
	acutifrons	Dark			Guanine				13
	(spec.)	Dark	483						20
Evermanella	indica	Dark	484						21
Omosudis	lowei	Dark			Guanine		65/*60*	250/*250*	22

adaptation the incident light is focused mainly onto the cone outer segments with an increase of the incident light intensity by more than 500% (the simulation was made for a two-dimensional arrangement; in the real 3D situation, the factor is certainly even higher) (Fig. 15B). This mechanism works particularly well for long wavelengths whereas it is less effective for short wavelengths (Fig. 15E–H; *cf.* Figs. 7D and 14E). As already mentioned, this seems well adjusted to the red-sensitive cone photopigment (Fig. 7D) and the predominantly long-wavelength ambient light. While light levels for the cones at the bottom of the cup are amplified, the disordered phase of guanine crystallites underneath the cup further attenuate the light leaking through the bottom of the cup, so that only a very small fraction of light reaches the rods there (Kreysing et al., 2012) (Fig. 15B, E-H). The combined effect of this arrangement is that both the less sensitive cones and the very sensitive rods receive appropriate amounts of light to allow their simultaneous operation at intermediate light levels, which prevail in the dim habitat of the fish.

Second, even in the dark-adapted retina where the tapetal cup widens at the bottom such that the 'parabolic mirror' ceases to exist (cf. Fig. 10B, D, F), the arrangement of guanine crystals still provides remarkable increase of incident light intensity (Fig. 15C). However, the 'focus level' is less sharp than in the light-adapted condition; rather, elevated light intensities are present over a larger depth range of the photoreceptor bundle. This fits well with the situation that now both rod and cone outer segments are crowded together at this level, and occupy a wider depth range (inset of Fig. 15C; cf. also Fig. 10F); thus, both types of photoreceptor cells seem equally illuminated and the rods can work in the dark environment.

Third, the role of the multilayer-forming lamellar platelets is elucidated. Much of the focusing and amplifying effects shown in Fig. 15B are achieved by this multilayer alone; when the irregular crystals are omitted in the simulation, the results are almost the same (not shown). By contrast, the increased light intensity in the 'open' cup (*i. e.*, without the parabolic shape) is mostly due to the irregular crystals: removing the multilayer from the simulation fails to change the results conspicuously (Fig. 15D *vs.* 15C). This means that even the 'simple cups' may provide a considerably enhanced light intensity, at least for the cones.

5.2. Estimates for other fish with different types of grouped retinae and cups

Apart from *G. petersii*, there is still a lack of reliable quantitative data on the ultrastructure (e. g., thickness and spacing of the platelets) and on the spectral sensitivities of the photopigments of most of the fishes with grouped retinae and tapetal cups (Table 2). However, some conclusions about the function of their cups appear to be feasible.

The striking structural and even ultrastructural similarities between all retinae of Osteoglossiformes studied so far (Figs. 3A–D, 4A–D, 6D–G; Table 2) may suggest that their cups have a similar function and provide the fish with similar behavioral advantages as *Gnathonemus* (*cf.* also Section 6). Even the 'simple cups' with strongest deviations from ideal parabolic mirrors as found in fishes such as the Percidae and Clupidae, may serve similar purposes (Fig. 15D).

The situation is different in the retinae of deep-sea fishes where no mixed rod-and-cone bundles exist. In these retinae, only bundles of rods are surrounded by tapetal cups (Fig. 3E–G). Although the available data do not allow for a completely reliable simulation, it is more than an intuitive guess to assume that these cups provide increased light intensities for the rods, similarly as shown in Fig. 15B (but, of course, with an optimum in the short range of

wavelengths; *cf.* Fig. 7E–G). In fact, the assumption of enhanced light delivery by these tapetal cups appears to justified since (i) even the 'simple cups' tend to increase local light intensities significantly (Fig. 15D) and (ii) in deep-sea fish with tubular eyes, rod bundles in tapetal cups occur even in the accessory retina which is located very close to the lens (e.g., Locket, 1971, 1977) such that no focused image can occur; it may be speculated that extremely dim light signals can be caught there, to trigger appropriate behavioral reactions (e.g., to swim closer for inspection of the object by the main retina).

In addition, some deep-sea fish retinae also contain tapetal cups for single outer segments, mostly of cones (Fig. 4E–F). These are dissimilar to the 'parabolic mirror-like' cups simulated in Fig. 15. In addition to guanine multilayers closely surrounding the individual outer segment, another important component seems to be a quarter-wave stack of flat platelets at the bottom of each single-outer-segment cup (i. e., 'behind' the outer segments with respect to the incident light; Fig. 4F). Also in this case, simulations reveal some peculiarities in the functioning of the cups.

These guanine-surrounded cavities are only a few wavelengths wide and only barely display a conical shape that would give rise to a confinement of wavefronts. Nonetheless, light intensities in such a half-open cavity seem to be greatly increased over the incident level. Conservative estimates inferred from two-dimensional FDTD simulations show an average light intensification in excess of 3.5. The reason for this unexpected high value is probably twofold. First, the incident light is efficiently hindered from leaving the cavity in lateral direction by the surrounding guanine multilayer hit under a steep angle (Fig. 4E) before being back-reflected by the densely spaced multilayer at the bottom of the cup (Fig. 4F). Second, light that penetrates the disordered phase of guanine next to a single-segment cup is randomized in the propagation direction and has a high chance of penetrating the lateral 'guanine wall' and thus to enter the space occupied by the outer segment. The situation of the outer segment is thus similar to that of a detector inside an (half-open) integrating sphere.

As a consequence of this arrangement, light is not focused within a narrow range (as in the 'parabolic mirrors', cf. Fig. 15B, E–H) but rather evenly distributed along the length of the cone outer segments (Fig. 16A). This should allow an effective light absorption by virtually all discs within a given outer segment. Furthermore, assuming a quarter-wave multilayer stack with 65 nm thick guanine platelets (Frederiksen, 1976), maximum light reflectivity is achieved in the short range of the light spectrum, at about 400–500 nm (Fig. 16B–D); this is known to fit well to the putative absorption maxima of deep-sea fish cones and to the wavelengths of the available light (*cf.* Fig. 7E–G). Commonly used analytical multilayer reflectivity calculations (*cf.* Land, 1972) revealed only a slight blue shift in the spectral maximum when light arrives obliquely to the axis of the outer segment (Fig. 16C). More strikingly, the regularity of thickness and spacing of guanine platelets at the bottom of the cup seems to be critical for proper functioning of these cups. In fact, a small degree of spatial noise might even increase the overlap between the absorption spectrum of the photopigment and the reflection characteristics of the multilayer (Fig. 16B), especially for rather broadly absorbing pigments centered around 470 nm to 490 nm (*white line* in Fig. 16B; *cf.* Table 2 and Fig. 7G). Taken together, the single-outer-segment cups of deep-sea fishes are apparently optimized for the needs of the fish.

6. Physiological and behavioral impact of the retinal specialization

The above-mentioned anatomical data and the mathematical simulations allow for some predictions in respect to the visual capabilities of the fish. In fact, these predictions have been verified by electrophysiological and behavioral experiments on *Gnathonemus petersii* (Kreysing et al., 2012). The basic 'disadvantage' of the macroreceptors in the grouped retina is its strikingly low spatial resolution of 30–50 μm at the level of retina (Fig. 12C) which corresponds to about 3° of visual angle (Schuster and Amtsfeld, 2002; Landsberger et al., 2008; Kreysing et al., 2012). It means that the fish cannot detect any features smaller than six times the diameter of the full moon as viewed from earth. Another apparent disadvantage is that, if only one spectral type of cones exists (Fig. 7D) and the signals from cones and rods are pooled (Fig. 11A, B), the fish should be color-blind. However, it has been shown that these apparent disadvantages, when considered in the habitat of the fish, turn into advantages (see below).

6.1. Electrophysiological studies in Gnathonemus petersii

Recordings of the electroretinogram (ERG) and of the activities of single units in the optic tectum of the fish revealed that in fact, as proposed from the above-mentioned considerations (e.g., Fig. 15A and B) (i) the green-sensitive rods contribute to the light-adapted ERG (rather than being saturated as in 'conventional' retinae) (Fig. 17A) and (ii) rods and cones displayed the same range of light intensity responsiveness (Fig. 17B) (Kreysing et al., 2012). This was also supported by the results of behavioral tests (optomotor responses – see Section 6.2) revealing that both rods and cones contribute to the responses of the fish to a moving pattern of stripes (Fig. 17C).

Another prediction is that strong signal convergence and pooling of information from large groups of rods and cones should reduce the time required for information processing (Warrant, 1999). Indeed, recording from single neuronal units – presumed to reflect afferent input to the tectum – from *Gnathonemus petersii* revealed that the neurons can detect signals with higher temporal frequency and at lower contrast than those of *Carassius auratus*, a fish with a conventional retina allowing for high spatial resolution and color vision (Fig. 17D).

6.2. Comparative behavioral tests in Gnathonemus petersii

Three different paradigms were used to perform behavioral tests in response to visual stimuli (Kreysing et al., 2012). First, so-called startle reactions were studied by applying a visual stimulus (circle) which rapidly expands in size. This mimics the silhouette of an approaching predator, and triggers a flight reaction of the fish away from the stimulus. Second, optomotor responses were monitored; in these experiments, a moving stripe pattern was projected onto the bottom of the fish tank and it was assessed whether the fish follow the movements of the pattern. In these experiments, the brightness contrast and the width of the stripes were variable, as well as the velocity of the movement of the pattern. Third, choice experiments were carried out; the fish were trained in a two-alternative forced-choice procedure to swim toward a projected visual simulus (circle or square) of variable size. These latter experiments confirmed that spatial resolution is so poor in *Gnathonemus* that the fish cannot see objects smaller than about 3° visual angle, no matter whether these objects are stationary or moving (Fig. 18A).

However, the impact of the specialized retina structure of *Gnathonemus petersii* can be most clearly revealed if experiments are designed which mimic the natural conditions under which the fish are living, i.e., when the effects of visual stimuli with a low signal-to-noise ratio are applied. The fact that *Gnathonemus* cannot see small objects should provide the fish with a noise-rejection filter that might benefit them in their fast flowing natural habitats, where water turbidity often is caused by a high density small

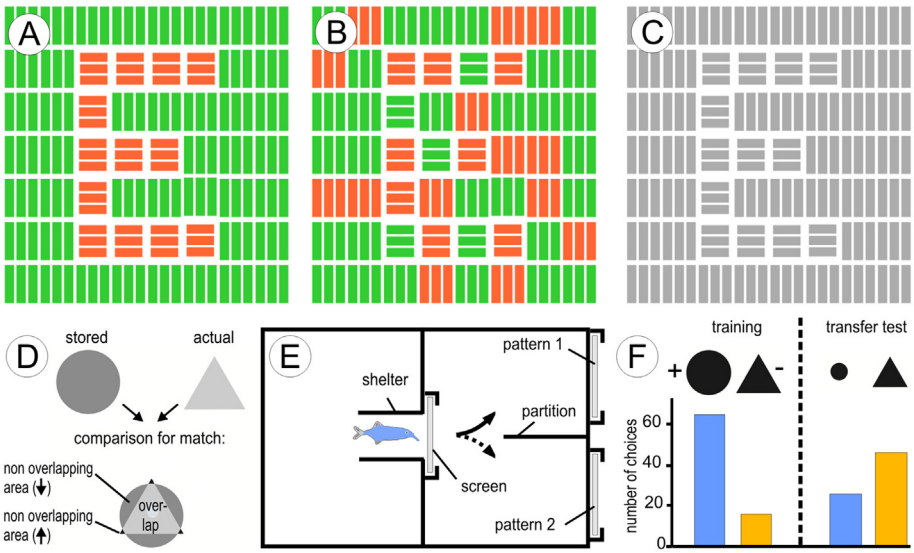

Fig. 19. **A**–**C**, Advantage of missing color discrimination. Color-camouflaged visual signals (**B**) cannot be easily detected by trichromates but are quickly identified by deuteranopic or completely color-blind individuals (**C**). **D**–**F**, Use of template matching to memorize visual objects by *Gnathonemus*. **D**, Template matching is a strategy to identify a memorized (stored) visual object by comparing it with an actually presented object; this is 'identified' if overlap is pronounced and the non-overlapping areas are small. **E**, Experimental setup. A fish views two patterns through a transparent screen from a fixed vantage point in its daytime shelter. It was trained to swim to one of the two patterns (circle) when the screen was lifted, to receive a reward. Then, tests were made in which the fish faced not the original patterns but novel appropriately chosen ones. **F**, The outcome of these tests showed that the fish did not recognize the circle as such or as something that does not contains edges. (D–F, modified from Schuster and Amtsfeld, 2002).

floating particles such as plant material or other organic or inorganic matter (Moritz, 2010; Ogbeibu and Ezeunara, 2002; Tawari-Fufeyin and Ekaye, 2007). To prove this prediction, *G. petersii* - and, in comparison, *Lepomis gibbosus* and *C. auratus*, two diurnal visual specialists (Hairston et al., 1982; Neumeyer et al., 1991) – were tested for their capability to detect an object under "noisy" conditions (Kreysing et al., 2012).

Indeed these experiments revealed that the fish tolerate a much lower signal-to-noise ratio than *C. auratus* or *L. gibbosus*; this was shown for low intensity differences between stimulus and background (Fig. 18B), for color-camouflaged stimuli (Fig. 18C), and for the overlay of signals with gray noise, in startle reactions (Fig. 18D) and optomotor responses (Fig. 18E) as well as in choice experiments (Fig. 18F and G) (Kreysing et al., 2012).

The starting point for testing color pooling was the observation that the elephantnose fish can equally well as goldfish be startled with rapidly expanding black circles, shown before a white background. Moreover, the response can also be elicited by expanding solid green and red circles chosen such as to lead to the same response probability in both species. This motivated the following mimic of Mollon's experiments on deuteranopes. An equal number of red and green pixels (with spectra as in the previous experiments) were displayed on a screen. The pixels were dynamic, i.e. each pixel appeared at a randomly assigned position and disappeared after a randomly assigned lifetime, taken from a gaussian distribution, while another pixel of the same color appears at another location. This setting can be programmed to define an expanding circle not from brightness or color contrast but from the lifetime of pixels inside it. Otherwise the expansion dynamics (initial and maximal size of the circle, speed of expansion) of this virtual circle can be chosen just as with real expanding circles. Within the virtual circle the red and green circles were frozen whereas they were quickly exchanged outside, with an average pixel-lifetime much shorter than the duration of expansion of the circle. Fig. 18C shows that *Gnathonemus* is significantly better at detecting the expanding virtual circle than goldfish, probably reflecting the advantage of missing color discrimination (i. e., 'color pooling') (cf. Fig. 19A–C).

A particularly interesting observation was made when the fish were trained in a two-alternative forced-choice procedure to swim toward a projected large black square (6.2° visual angle; *insets* in Fig. 18F and G). After the fish had learned this task, the visual contrast of the square was reduced stepwise until the fish could no longer detect the object, indicated by a performance of 50% correct choices (chance level). Under normal conditions, when no noise was added, both species reached the 50% chance level at about the same contrast level (Fig. 18F, G). However, when small moving noise particles were covering the screen with the large square, the two species behaved dramatically different. While *Gnathonemus* was not affected at all by the addition of the small noise particles and reached a very similar detection efficiency of the large object, the *Lepomis* were extremely disturbed by the moving noise particles; they swam agitatedly and refused to approach the screen. By contrast, *Gnathonemus* (which could not see the small moving particles) were not frightened by them and were still able to detect the large object behind this veil of noise (Fig. 18F, G) (Kreysing et al., 2012).

In this context it is noteworthy that while we (or at least, most of us) are used to enjoying the advantages of color vision, in some instances it can be advantageous to be color-blind. This is exemplified in Fig. 19A–C which demonstrates, according to the psychophysiological experiments of Mollon's group (Morgan et al., 1992), that trichromates can quickly identify a letter if its color differs from that of the background (Fig. 19A) or if it is built by uncolored symbols of different orientation (Fig. 19C) but need more time to identify the color-camouflaged letter (Fig. 19B). By contrast, this is no problem for human deuteranopes or completely color-blind individuals.

Despite of the above-mentioned behavioral advantages of the grouped retina it is obvious that the fish should be handicapped by the bad spatial resolution of its vision when a visual object must be memorized. It is remarkable that *Gnathonemus* is one of the few vertebrates and the only fish known so far to employ what is probably the most basic strategy to memorize a visual object: template matching (Schuster and Amtsfeld, 2002). This recognition strategy disposes of any actual analysis of the image such as the

detection of edges or other image elements. Rather, it simply stores an interesting object as a 'snapshot' of the retinal image, taken at a given vantage point. The recognition process consists of classifying the degree of spatial overlap a current retinal image has with the stored snapshot (Fig. 19D). While this simple mechanism does not require much further neuronal processing it comes at the cost of a lack in viewpoint invariance: seen from a greater than the snapshot distance the image of a given object may overlap very little with the snapshot, while a closer, but completely different object, may overlap better. Despite its shortcomings template matching can be a very clever strategy when combined with behaviors that ensure the comparison between stored and actual image is made only close to that vantage point at which the snapshot was taken. Fig. 19E–F shows experiments and critical tests that demonstrated the use of such a simple strategy in the elephantnose fish and that make it not likely that the fish uses higher strategies to analyze the image (Schuster and Amtsfeld, 2002).

In these experiments, it was tested whether indeed the fish classifies similarity simply according to the degree of retinal overlap of the actual image with the stored snapshot. This predicts a rather odd but experimentally testable consequence: Rescaling the sizes of the original circle and the triangle such that they both overlap equally well with the snapshot should cause the fish to equally choose the two objects. Moreover, the preference should even be reversed by making a rescaled version of the unrewarded object overlap better with the snapshot (Fig. 19E). Both predictions were met.

These and similar tests (Schuster and Amtsfeld, 2002) clearly showed that *Gnathonemus* uses a basic strategy previously known from insects. Bees and wasps successfully use such strategies for instance to find the entrance to a nest (e.g. Cartwright and Collett, 1983; Zeil, 1993; Collett, 1995). Part of their successful application is that they store views taken from a limited number of viewpoints taken on a defined path which they also follow on their returns. The way mormyrids combine template matching with locomotor strategies is still unknown but a 'shelter hopping' strategy was proposed (Schuster and Amtsfeld, 2002). According to this hypothesis, the fish would start its route from a defined daytime hiding place from which the distance and viewing angle of distant landmarks would be fixed. The landmarks would then guide the fish's course to the next hiding place and so on.

In summary, the behavioral findings make it unlikely that the fish use more advanced strategies of image processing; this fits well with the coarse image resolution of the fish and with the summation of receptor contributions within the bundles (Kreysing et al., 2012).

7. Structure and function of grouped retinae - emerging general rules

Based upon the results obtained in *Gnathonemus petersii* and upon data known from other fishes with grouped retinae and/or tapetal cups (Tables 1 and 2; Figs. 3 and 4), some reasonable predictions appear to be possible about the behavioral benefits of this specialized retina in general. Very probably, both the retinal structure and its behavioral advantages are very similar among all Osteoglossiformes (cf. Table 1, first group on top). Apparently all these fishes, living in turbid waters, possess platelet-covered duplex cups, and thus should profit from pooling of rod and cone signals (Figs. 11, 15, 17 and 18) in a similar way as *Gnathonemus* does. Very probably, their maximum spectral sensitivities lie at some 535 up to >615 nm, such that they can detect the red light which predominates in turbid waters (Fig. 7C).

All the Aulopeiformes (cf. Table 1, last group on bottom), living in the darkness of the deep-sea, must rely upon the blue light which either penetrates the depth of the water or is delivered by bioluminescence of other organisms (Fig. 7F). This is reflected by the expression of photopigments maximally sensitive to wavelengths of about 440–480 nm (Table 2) and by two types of specialized cups: rod-only cups and cone-only cups (Fig. 5). The thin platelets at the bottom of the cone-only cups maximally reflect short wavelengths (Fig. 16; cf. also Frederiksen, 1976). In these fishes, maximum gathering of the dim available light by the cups is the obvious purpose of the retinal specialization. The fish have a poor spatial visual resolution but might benefit from the fact that they cannot see small objects and thus can filter out small noise particles, still allowing them to see a large object such as a predator, even in turbid ('noisy') waters carrying lots of small particles.

In addition to these two well-defined groups, a number of other fishes also display grouped retinae, mostly with 'simple' tapetal cups (Table 1: Elopiformes, Clupeiformes, Perciformes, and Beryciformes) which, even if 'imperfect' as compared to those of the Osteoglossiformes, may provide considerable light collection (Fig. 15 D). This might enable these fishes to visit dark environments such as turbid waters of river deltas or deeper areas of the sea. Noteworthy, some Clupeiformes appear to possess, in dependence on retinal topography, both tapetal cups comparable to the rod-only cups of the deep-sea fishes and tapetal 'curtains' supporting the detection of polarized light (Heß et al., 2006; Novales Flamarique, 2011) (Figs. 4D, 3H–K). Whereas the latter function is of obvious use for the migrating behavior of the herrings, it is difficult to speculate about the reason(s) why the lesser weever fish (*Trachinus vipera*) has a grouped retina but no tapetal cups. This is particularly difficult to understand because in all other cases, the ontogenetic appearance of the photoreceptor grouping coincides with that of the reflective cups (Fig. 6), and because a decrease of spatial resolution (cf. Fig. 12) without compensation by maximum light collection is hardly understandable. A possible hypothesis is that the fish emerged from epipelagic ancestors with tapetal cups, and then got rid of the tapetum when they occupied coastal waters where too much light may be disturbing.

In summary, tapetal cups are a retinal specialization of various Teleostian fishes. They are higly reflective structures that minimize the threshold of the enclosed photoreceptors, even adjusted to their spectral sensitivity. In contrast to the cone-only cups of some deep-sea fish specifically 'illuminating' a single cone, the other ('parabolic mirror-like') cups provide amplified light intensities to groups of (many) photoreceptors. This must result in decreased spatial resolution of vision; however, this is no problem in the case of rod-only cups (because the signals from many rods are pooled anyway by the retinal circuits) and is even advantageous for fishes with duplex cups living in turbid water (because the disturbing noise signals are filtered out). In the latter case, the cups generate a matched sensitivity of rod and cone photoreceptors, and thus facilitate the detection of low-contrast and color-mixed stimuli, within the dim, turbid habitat of the fish. In any case, the behavioral advantages of this highly complex specialization appear to justify the developmental (and metabolic) costs necessary for their installation and maintenance.

Acknowledgments

The authors wish to thank Peter Bartsch (Berlin) for expert help on the phylogeny of fishes, Ms Barbara Bauch (Bonn) and Jens Grosche (Leipzig: *www.effigos.de*) for their contributions to the graphics, Meik Landsberger (Bonn) for sharing some of his data on training experiments with *G. petersii*, and Tapas C. Nag (New Delhi) for providing images and data on *Notopterus notopterus*. Particular thanks are due to Jean-Pierre Denizot who provided *Mormyrus rume proboscirostris* fish of different developmental stages. AM wants to thank Russell D. Fernald (Stanford) for providing the T7 antibody. The authors also wish to thank the Deutsche Forschungsgemeinschaft (RE 849/11 to AR, Schu 1470/3 to SS, WA 348/

24 to H-JW, Excellence Cluster 277 “Cognitive Interaction Technology”to JE and RP, Em 43/12 to GvdE) and the Friedrich-Ebert-Stiftung (to RP) for support of research. The work presented was kindly supported by funding from the German Federal Ministry of Education and Research (BMBF, 1315883 to MF and AK).

References

Ali, M.A., Anctil, M., 1976. Retinas of Fishes. AN Atlas. Springer, Berlin, pp. 1–284.
Awaiwanont, K., Gunarso, W., Sameshima, M., Hayashi, S., Kawamura, G., 2001. Grouped, stacked rods and tapeta lucida in the retina of Japanese anchovy Engraulis japonicus. Fischeries Sci. 67 (5), 804–810.
Best, A.C.G., Nicol, J.A.C., 1979. On the eye of the Goldeye Hiodon alosoides (Teleostei: hiodontidae). J. Zool. 188 (3), 309–332.
Braekevelt, C.R., 1982. Fine structure of the retinal epithelium and retinal tapetum lucidum of the goldeye Hiodon alosoides. Anat. Embryol. (Berl) 164 (2), 287–302.
Braekevelt, C.R., McIntyre, D.B., Ward, F.J., 1989. Development of the retinal tapetum lucidum of the walleye (Stizostedion vitreum vitreum). Histol. Histopathol. 4 (1), 63–70.
Brauer, A., 1906. Die Tiefseefische. Ii. Anatomischer Teil. In: Chun, Carl (Ed.), Wissenschaftliche Ergebnisse der Deutschen Tiefsee-Expedition auf dem Dampfer 'Valdivia' 1898-1899, vol. 15. Gustav Fischer Verlag, Jena, pp. 164–197. Tables XXXI-XXXIV.Retinomotor pigment migration in the teleost retinal pigment epithelium. II. Cyclic-3',5'-adenosine monophosphate induction of dark-adaptive movement in vitro.
Burnside, B., Wang, E., Pagh-Roehl, K., Rey, H., 1993. Retinomotor movements in isolated teleost retinal cone inner-outer segment preparations (CIS-COS): effects of light, dark and dopamine. Exp. Eye Res. 57 (6), 709–722.
Cartwright, B.A., Collett, T.S., 1983. Landmark learning in bees. Experiments and models. J. Comp. Physiol. 151, 521–543.
Collett, T.S., 1995. Making learning easy: the acquisition of visual information during orientation flights of solitary wasps. J. Comp. Physiol. A. 177, 737–747.
Collin, S.P., Hoskins, R.V., Partridge, J.C., 1998. Seven retinal specializations in the tubular eye of the deep-sea pearleye, Scopelarchus michaelsarsi: a case study in visual optimization. Brain Behav. Evol. 51 (6), 291–314.
Connaughton, V.P., Graham, D., Nelson, R., 2004. Identification and morphological classification of horizontal, bipolar, and amacrine cells within the zebrafish retina. J. Comp. Neurol. 477, 371–385.
Darwin, C., 1859. On the Origin of Species by Means of Natural Selection, or the Preservation of Favoured Races in the Struggle for Life, first ed. John Murray, London.
Davis, M.P., Fielitz, C., 2010. Estimating divergence times of lizardfishes and their allies (Euteleostei: Aulopiformes) and the timing of deep-sea adaptations. Mol. Phylogenet. Evol. 57 (3), 1194–1208.
Dearry, A., Burnside, B., 1984. Effects of extracellular Ca^{++}, K^{+}, and Na^{+} on cone and retinal pigment epithelium retinomotor movements in isolated teleost retinas. J. Gen. Physiol. 83 (4), 589–611.
Denton, E.J., Nicol, J.A.C., 1965. Reflexion of light by external surfaces of the herring, Clupea harengus. J. Mar. Biol. Ass. 45 (03), 711–738.
Douglas, R.H., Partridge, J.C., 1997. On the visual pigments of deep-sea fish. J. Fish. Biol. 50 (1), 68–85.
Douglas, R.H., Partridge, J.C., Marshall, N.J., 1998. The eyes of deep-sea fish. I: lens pigmentation, tapeta and visual pigments. Prog. Retina Eye Res. 17 (4), 597–636.
Engström, K., 1963. Cone types and cone arrangements in teleost retinae. Acta Zool. 44 (1–2), 179–243.
Enoch, J.M., 1980. Vertebrate receptor optics and orientation. Doc. Ophthalmol. 48 (2), 373–388.
Fechler, K., Holtkamp, D., Neusel, G., Sanguinetti-Scheck, J.I., Budelli, R., von der Emde, G., 2012. Mind the gap: the minimal detectable separation distance between two objects during active electrolocation. J. Fish Biol. 81, 2255–2276.
Franz, V., 1921. Zur mikroskopischen Anatomie der Mormyriden. Zool. Jahrb., Abt. Allgem. Zool. Physiol. Tiere 42, 91–146.
Frederiksen, R.D., 1976. Retinal tapetum containing discrete reflectors and photoreceptors in the bathypelagic teleost Omosudis lowei. Vidensk Meddr Dansk Naturh Foren 139, 109–146.
Garten, S., 1907. Die Veränderungen der Netzhaut durch Licht. In: Gräfe, A., Sämisch, Th (Eds.), Handbuch der gesamten Augenheilkunde, 2. Aufl., Bd. III. Engelmann, Leipzig, pp. 1–250.
Hairston Jr., N.G., Li, K.T., Easter Jr., S.S., 1982. Fish vision and the detection of planktonic prey. Science 218 (4578), 1240–1242.
Hein, S.A.A., 1913. Over oogleden en fornices conjunctivae bij tetostomi. Tijds. D. Nederl Dierk. Vereen, Ser. 2 (Dl.12), 238–280 (cited from Walls, G.L., 1963. The vertebrate eye and its adaptive radiation, 2nd ed. Hafner Publishing Company Cra, New York.).
Heß, M., Melzer, R.R., Eser, R., Smola, U., 2006. The structure of anchovy outer retinae (Engraulididae, Clupeiformes) – a comparative light- and electron-microscopic study using museum-stored material. J. Morphol. 267 (11), 1356–1380.
Hopkins, C.D., 2009. Electrical perception and communication. In: Squire, L.R. (Ed.), Encyclopedia of Neuroscience, vol. 3. Academic Press, Oxford, pp. 813–831.
Johns, P.R., 1982. Formation of photoreceptors in larval and adult goldfish. J. Neurosci. 2 (2), 178–198.
Kirk, J.T.O., 1985. Effects of suspensoids (turbidity) on penetration of solar radiation in aquatic ecosystems. Hydrobiologia 125 (1), 195–208.
Kondrashev, S..L., Gnyubkina, V.P., Zueva, L.V., 2012. Structure and spectral sensitivity of photoreceptors of two anchovy species: Engraulis japonicus and Engraulis encrasicolus. Vis. Res. 68, 19–27.
Kreysing, M., Pusch, R., Haverkate, D., Landsberger, M., Engelmann, J., Ruiter, J., Mora-Ferrer, C., Ulbricht, E., Grosche, J., Franze, K., Streif, S., Schumacher, S., Makarov, F., Kacza, J., Guck, J., Wolburg, H., Bowmaker, J., von der Emde, G., Schuster, S., Wagner, H.-J., Reichenbach, A., Francke, M., 2012. Photonic crystal light collectors in fish retina improve vision in turbid water. Science 336 (6089), 1700–1703.
Kunz, Y.W., Ni Shuilleabhain, M., Callaghan, E., 1985. The eye of the venomous marine teleost Trachinus vipera with special reference to the structure and ultrastructure of visual cells and pigment epithelium. Exp. Biol. 43 (3), 161–178.
Lamb, T.D., Collin, S.P., Pugh Jr., E.N., 2007. Evolution of the vertebrate eye: opsins, photoreceptors, retina and eye cup. Nat. Rev. Neurosci. 8 (12), 960–976.
Land, M.F., 1972. The physics and biology of animal reflectors. Prog. Biophys. Mol. Biol. 24, 75–106.
Land, M.F., Nilsson, D.-E., 2002. Animal Eyes. Oxford University Press, pp. 1–221.
Landsberger, M., Emde, G.v.d., Haverkate, D., Schuster, S., Gentsch, J., Ulbricht, E., Reichenbach, A., Makarov, F., Wagner, H.-J., 2008. Dim light vision – morphological and functional adaptations of the eye of the mormyrid fish, Gnathomenus petersii. J. Physiol. Paris 102 (4–6), 291–303.
Laties, A.M., Enoch, J.M., 1971. An analysis of retinal receptor orientation. I. Angular relationship of neighboring photoreceptors. Invest. Ophthalmol. Vis. Sci. 10 (1), 69–77.
Locket, N.A., 1971. Retinal anatomy in some scopelarchid deep-sea fishes. Proc. R. Soc. Lond. B Biol. Sci. 178 (51), 161–184.
Locket, N.A., 1977. Adaptations to the deep-sea environment. In: Crescitelli, F. (Ed.), The Visual System in Vertebrates, Handbook of Sensory Physiology, VII/5. Springer, Heidelberg, pp. 67–122.
Mack, A.F., 2007. Evidence for a columnar organization of cones, Müller cells, and neurons in the retina of a cichlid fish. Neuroscience 144 (3), 1004–1014.
Masland, R.H., 2012. The neuronal organization of the retina. Neuron 76 (2), 266–280.
McEwan, M.R., 1938. A comparison of the retina of the mormyrids with that of various other teleosts. Acta Zool. 19 (3), 427–465.
Michaelson, I.C., 1954. Retinal Circulation in Man and Animals. Charles C. Thomas, Springfield, pp. 1–146.
Moller, P., 1995. Electric Fishes: History and Behavior, first ed. Chapman & Hall, London, New York.
Moller, P., Serrier, J., Belbenoit, P., Push, S., 1979. Notes on ethology and ecology of the Swashi River mormyrids (Lake Kainji, Nigeria). Behav. Ecol. Sociobiol. 4 (4), 357–368.
Moore, G.A., 1944. The retinae of two north American teleosts, with special references to their tapeta lucida. J. Comp. Neurol. 80 (3), 369–379.
Morgan, M.J., Adam, A., Mollon, J.D., 1992. Dichromats detect colour-camouflaged objects that are not detected by trichromats. Proc. Biol. Sci. 248 (1323), 291–295.
Moritz, T., 2010. Fishes of Iguidi River - a small forest stream in South-East Benin. Ichthyol. Explor. Freshwaters 21 (1), 9–26.
Munk, O., 1966. Ocular anatomy of some deep-sea teleosts. In: The Carlsberg Foundation's Oceanographical Expedition Round the World 1928-30 and Previous “Dana” Experditions. Andr. Fred. Høst & Søn, Copenhagen, pp. 5–65. Dana-Report no. 70.
Munk, O., 1975. On the eyes of two notosudid teleosts, *Scopelosaurus hoedti* and *Abliesaurus berryi*. Vidensk Meddr Dansk Naturh Foren 138, 87–125.
Munk, O., 1977. The visual cells and retinal tapetum of the foveate deep-sea fish Scopelosaurus lepidus (Teleostei). Zoomorphology 87 (1), 21–49.
Munk, O., 1989. Duplex retina in the mesopelagic deep-sea teleost Lestidops affinis (Ege, 1930). Acta Zool. 70 (3), 143–149.
Nag, T.C., 2004. The retinal pigment epithelium of the teleost Notopterus notopterus (Pallas): appearance of basal infoldings during prolonged dark-adaptation. Histol. Histopathol. 19 (1), 143–150.
Nelson, J.S., 2006. Fishes of the World, fourth ed. John Wiley, Hoboken, NJ.
Neumeyer, C., Wietsma, J.J., Spekreijse, H., 1991. Separate processing of "color" and "brightness" in goldfish. Vis. Res. 31 (3), 537–549.
Novales Flamarique, I., 2011. Unique photoreceptor arrangements in a fish with polarized light discrimination. J. Comp. Neurol. 519 (4), 714–737.
Nwani, C.D., Odoh, G.E., Ude, E.F., Okogwu, O.I., 2011. Food and feeding habits of Gnathonemus pertersii (Osteichthyes: Mormyridae) in Anambra River, Nigeria. Int. Aquat. Res. 3, 45–51.
O'Connell, C.P., 1963. The structure of the eye of Sardinops caerulea, Engraulis mordax, and four other pelagic marine teleosts. J. Morphol. 113 (2), 287–329.
Ogbeibu, A.E., Ezeunara, P.U., 2002. Ecological impact of brewery effluent on the Ikpoba River, Nigeria, using the fish communities as bio-indicators. J. Aquat. Sci. 17 (1), 35–44.
Ogbeibu, A.E., Ezeunara, P.U., 2005. Studies on the food composition and feeding pattern of fish communities in the Ikpoba River, Southern Nigeria. J. Aquat. Sci. 20 (2), 117–129.
Okedi, J., 1965. The biology and habits of the mormyrid fishes: Gnathonemus longibarbis, Gnathonemus victoriae, Marcusenius grahami, Marcusenius nigricans, Petrocephalus catostoma. J. Appl. Ecol. 2 (2), 408–409.

Okedi, J., 1968. Notes on the Behaviour of the Small Mormyrid Fishes of Lake Victoria. Freshw. Fish. Org., Afr. Quest, Ann. Rep, pp. 42–48.
Partridge, J.C., Archer, S.N., Vanoostrum, J., 1992. Single and multiple visual pigments in deep-sea fishes. J. Mar. Biol. Ass. U.K 72 (1), 113–130.
Paugy, D., Traore, K., Diouf, P.S., 1994. Faune ichtyologique des eaux douces d'Afrique de l'Ouest. In: Teugels, G.G., Guegan, J.-F., Albaret, J.-J. (Eds.), Biological Diversity in African Fresh- and Brackish Water Fishes: Geographical Overviews: PARADI symposium = Diversité biologique des poissons des eaux douces et saumâtres d'Afrique: synthèses géographiques: symposium PARADI. ORSTOM, Paris.
Pointer, M.A., Carvalho, L.S., Cowing, J.A., Bowmaker, J.K., Hunt, D.M., 2007. The visual pigments of a deep-sea teleost, the pearl eye Scopelarchus analis. J. Exp. Biol. 210 (Pt 16), 2829–2835.
Pusch, R., Wagner, H.-J., von der Emde, G., Engelmann, J., 2013. Spatial resolution of an eye containing a grouped retina: ganglion cell morphology and tectal physiology of Gnathonemus petersii. J. Comp. Neurol..
Reichenbach, A., Robinson, S., 1995. Phylogenetic constraints on retinal organization and development: an Haeckelian perspective. Prog. Retin. Eye Res. 15 (1), 139–171.
Schultze, M., 1866. Zur Anatomie und Physiologie der Retina. Max Cohen & Sohn, Bonn.
Schuster, S., Amtsfeld, S., 2002. Template-matching describes visual pattern-recognition tasks in the weakly electric fish Gnathonemus petersii. J. Exp. Biol. 205 (Pt 4), 549–557.
Somiya, H., 1980. Fishes with eye shine: functional morphology of guanine type tapetum lucidum. Mar. Ecol. Progr. Ser. 2, 9–26.
Somiya, H., 1989. Guanine-Type retinal tapetum of three species of mormyrid fishes. Jpn. J. Ichthyol. 36 (2), 220–226.
Tawari-Fufeyin, P., Ekaye, S.A., 2007. Fish species diversity as indicator of pollution in Ikpoba River, Benin City, Nigeria. Rev. Fish Biol. Fish. 17 (1), 21–30.
Taylor, W.R., Smith, R.G., 2012. The role of starburst amacrine cells in visual signal processing. Vis. Neurosci. 29 (1), 73–81.
Taylor, S.M., Grace, M.S., 2005. Development of retinal architecture in the elopomorph species Megalops atlanticus, Elops saurus and Albula vulpes (Elopomorpha: Teleostei). Contrib. Mar. Sci. 37, 1–29.
Vaney, D.I., Taylor, W.R., 2002. Direction selectivity in the retina. Curr. Opin. Neurobiol. 12 (4), 405–410.
Virchow, H., 1882. Über die Glaskörper- und Netzhautgefäße des Aales. Morphol. Jahrb 7, 573–590.
Von der Emde, G., 1993. Capacitance discrimination in electrolocating, weakly electric pulse fish. Naturwissenschaften 80 (5), 231–233.
Von der Emde, G., Bleckmann, H., 1998. Finding food: senses involved in foraging for insect larvae in the electric fish Gnathonemus pertersii. J. Exp. Biol. 201 (Pt 7), 969–980.
Von der Emde, G., Behr, K., Bouton, B., Engelmann, J., Fetz, S., Folde, C., 2010. 3-Dimensional scene perception during active electrolocation in a weakly electric pulse fish. Front. Behav. Neurosci. 4, 26.
Von der Emde, G., Fetz, S., 2007. Distance, shape and more: recognition of object features during active electrolocation in a weakly electric fish. J. Exp. Biol. 210 (Pt 17), 3082–3095.
Wagner, H.-J., Ali, M.A., 1978. Retinal organization in goldeye and mooneye (Teleostei: hiodontidae). Rev. Can. Biol. 37 (2), 65–83.
Wagner, H.-J., 2007. Bipolar cells in the "grouped retina" of the elephantnose fish (Gnathonemus petersii). Vis. Neurosci. 24 (3), 355–362.
Walls, G.L., 1963. The Vertebrate Eye and Its Adaptive Radiation, second ed. Hafner Publishing Company Cra, New York.
Walmsley, R.D., Butty, M., Van der Piepen, H., Grobler, D., 1980. Light penetration and the interrelationships between optical parameters in a turbid subtropical impoundment. Hydrobiologia 70 (1–2), 145–157.
Warrant, E.J., 1999. Seeing better at night: life style, eye design and the optimum strategy of spatial and temporal summation. Vis. Res. 39 (9), 1611–1630.
Warrant, E.J., Locket, N.A., 2004. Vision in the deep sea. Biol. Rev. Camb. Philos. Soc. 79 (3), 671–712.
Zeil, J., 1993. Orientation flights of solitary wasps (Cerceris, Sphecidae, Hymenoptera). J. Comp. Physiol. A 172 (2), 189–205.
Zyznar, E., 1975. Tapeta lucida and the organisation of visual cells in teleosts. In: Ali, M.A. (Ed.), Vision in Fishes. Plenum Press, New York, pp. 299–304.
Zyznar, E.S., Ali, M.A., 1975. An interpretative study of the organization of the visual cells and tapetum lucidum of Stizostedion. Can. J. Zool. 53, 180–196.
Zyznar, E.S., Cross, F.B., Nicol, J.A.C., 1978. Uric acid in the tapetum lucidum of mooneyes Hiodon (Hiodontidae Teleostei). Proc. R. Soc. B: Biol. Sci. 201 (1142), 1–6.